New Mexico Geological Society Guidebook, 76th Fall Field Conference, 2026, p. 87–109, https://doi.org/10.56577/FFC-76.87

THIRD-DAY ROAD LOG:

RIO GRANDE VALLEY AND ALBUQUERQUE VOLCANOES

SEAN D. CONNELL[1], LARRY R. CRUMPLER[2], DANIEL J. KONING[1], FRASER GOFF[3], FRED M. PHILLIPS[3], AND SPENCER G. LUCAS[2]

[1]New Mexico Bureau of Geology and Mineral Resources, 801 Leroy Place, Socorro, NM 87801; sean.connell@nmt.edu
[2]New Mexico Museum of Natural History and Science, 1801 Mountain Road NW, Albuquerque, NM 87104
[3]Department of Earth and Environmental Science, New Mexico Institute of Mining and Technology, 801 Leroy Place, Socorro, NM 87801

Assembly Point: Parking lot for New Mexico Museum of Natural History and Science Annex (950 Eighteenth Street NW)
Departure Time: 7:30 AM
Distance: 26 miles
Stops: 3

Views, landmarks, and outcrops are given using the clock system, where 12:00 is straight ahead, 3:00 is to the right, and 9:00 is to the left. Driving distances are given in miles.

SUMMARY

The Day 3 agenda visits some of the numerous Pleistocene features of the Albuquerque area. Starting at an overlook of the Rio Grande valley, the group will discuss the Quaternary stratigraphy of the Rio Grande and hydrogeology of the Albuquerque Basin. The group will then use Interstate 25 to ascend West Mesa and the Llano de Albuquerque. The group will use Atrisco Boulevard to drive to the west side of the Albuquerque Volcanoes, where we will take a relatively easy 3–km (2-mi) hike, with less than 70 m (230 ft) of elevation change, in Petroglyph National Monument to examine volcanic features of Black Volcano. The trip ends with an optional stop at Boca Negra Canyon Day Use Area, on the east side of Petroglyph National Monument, where the group will examine an unusual feature of basaltic lava flows amid numerous petroglyphs.

7:30 AM: Depart New Mexico Museum of Natural History and Science Annex parking lot in caravan.

8:00 to 9:00 AM: Stop 1 discusses geomorphic features related to incision of the Rio Grande and the hydrogeology of the Albuquerque region.

9:30 to 11:30 AM: Stop 2 involves a hike into Petroglyph National Monument to examine volcanic features associated with the emplacement of the middle Pleistocene Albuquerque Volcanoes.

12:30 to 1:30 PM: Stop 3 is an optional stop to examine vesicle cylinders in lava flows at Boca Negra Canyon in Petroglyph National Monument.

1:30 PM: Trip ends.

Mileage Description *Distance to next entry*
[Waypoint, decimal degrees, World Geodetic System 1984]

0.0 **Waypoint 3.01 [N35.0976°, W106.6642°]**
Assemble caravan at north parking lot of New Mexico Museum of Natural History and Science Annex parking lot at 950 Eighteenth Street NW. The lot is located on nearly 24 m (80 ft) of latest Pleistocene and Holocene sedimentary fill associated with deposition of the Rio Grande during Holocene time.
Head west to parking lot exit, turning left (south) on to Eighteenth Street NW. ZERO ODOMETER AT THIS TURN. *0.1*

0.1 Turn right (west) onto Mountain Road NW. *0.3*

0.4 **Turn right at stoplight onto Rio Grande Boulevard NW and head north to I-40.** *0.1*

0.5 Hotel Albuquerque on right. Cross intersection with Bellamah Avenue. Move safely to left lane of Rio Grande Boulevard. *0.3*

0.8 Intersection of I-40 and Rio Grande Boulevard. Best Western Rio Grande Inn on left. On north side of the I-40 overpass, **turn left (west) and merge onto westbound I-40 on-ramp. Stay in right lane** for Frontage Road and Ouray Road exit a couple of miles ahead. *1.2*

2.0 Cross bridge across the Rio Grande. At 1:00 are the Adobe Cliffs, which are composed of sandy deposits of an approximately 34-m (110-ft)-thick alluvial and fluvial fill of the middle Pleistocene Los Duranes Formation (Connell et al., 2007; Raymond et al., 2010). *0.7*

2.7 **Exit I-40 at Coors Boulevard off-ramp (Exit 155). Keep right to Frontage Road**. *0.3*

3.0 **Turn right onto Ouray Road NW.** *0.2*

3.2 **Turn right onto Alamogordo Road NW.** *0.3*

3.5 **Turn left onto Bridges Avenue NW.** *0.1*

3.6 **Turn left onto Vista Grande Drive NW.** *0.2*

3.8 Park on Vista Grande Drive NW at entrance to West Bluff Park. Walk about 135 m (450 ft) east to shelter overlooking the Rio Grande (Fig. 3.01).

Waypoint 3.02 [N35.1098°, W106.6944°]

STOP 1. Historical Perspectives on the Rio Grande, Terrace Stratigraphy, and the Regional Aquifer System.

INTRODUCTION

This stop is located at West Bluff Park, which overlooks the Adobe Cliffs and the inner valley of the Rio Grande along the eastern margin of the Albuquerque Basin (Figs. 3.01 and 3.02). From this vantage, the rift-bounding Sandia Mountains dominate the eastern skyline, with the Manzanita and Manzano Mountains visible to the southeast. The park is developed on deposits of the Los Duranes Formation, a middle Pleistocene Rio Grande terrace.

At this stop, we discuss the geomorphic evolution of the Rio Grande valley and its relationship to the Santa Fe Group aquifer system (Figs. 3.03–3.05), river-terrace development, groundwater resources, and how geomorphic processes shaped the landscape and water resources of the Albuquerque area.



FIGURE 3.01 View to east of the city of Albuquerque, with the Rio Grande in the foreground and Sandia Mountains framing the skyline.

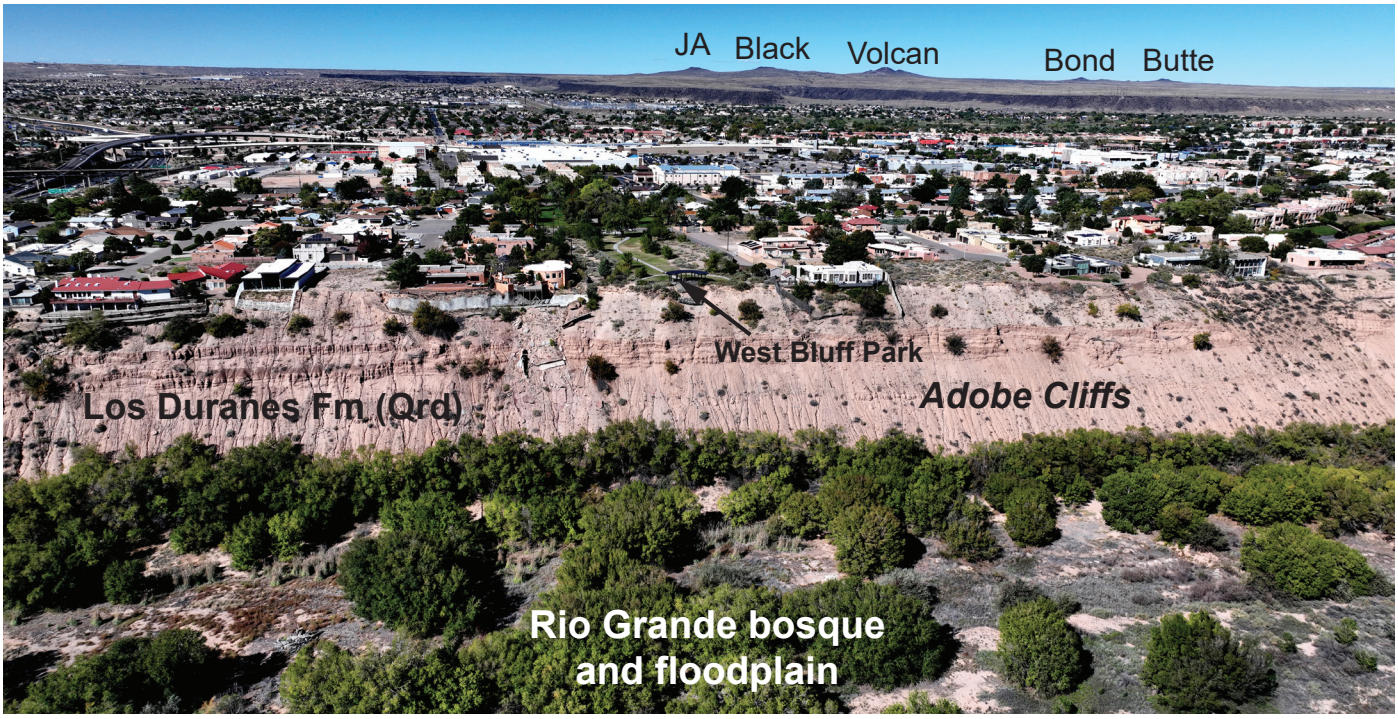


FIGURE 3.02. View to west of Los Duranes Formation (Qrd) and Segundo Alto terrace surface along the Adobe Cliffs. Peaks (cones) of the Albuquerque Volcanoes in background. Stop 1 is at the eastern edge of West Bluff Park.

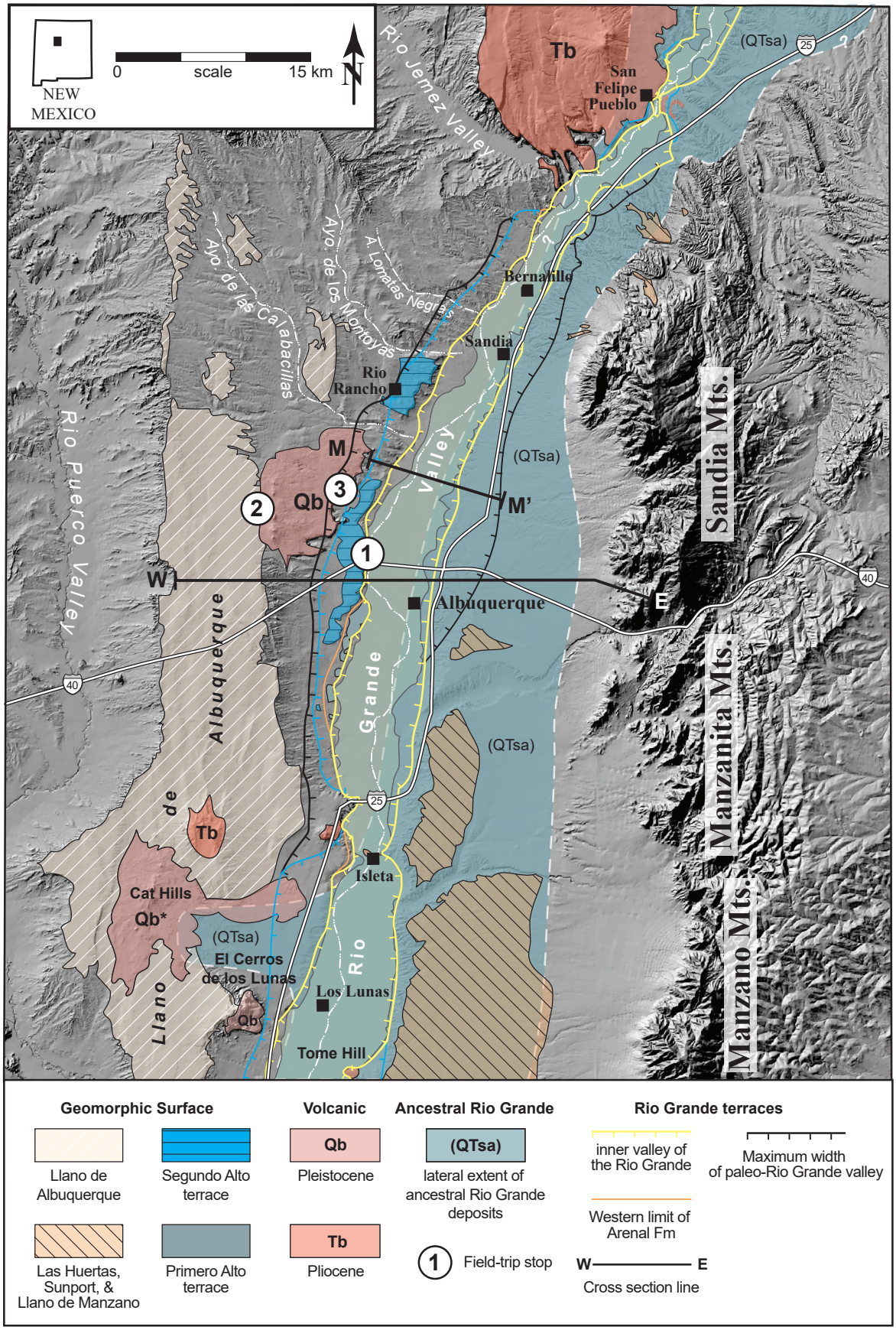


FIGURE 3.03. Major geomorphic features of the Albuquerque area (modified from Connell et al., 2007). White circle denotes Stop 1. Cross-section lines refer to Figures 3.04 and 3.09.

HISTORICAL PERSPECTIVES

This vantage provides an excellent view of the Rio Grande. The river today is not particularly large and is now a shadow of its former self. Prior to the construction of massive diversions for irrigation in San Luis Basin, Colorado, in the 1880s, the annual discharge of the Rio Grande was almost twice its current level (Phillips et al., 2011). The flow of the Rio Grande is now almost completely regulated, in great contrast to the enormous snow-melt floods that used to sweep down in the spring. The river is now shallow, narrow, and confined between levees. Before the river was engineered, the bed was as much as a mile wide, and laced with braided channels that could be quite deep in places. The river was home to large fish such as the shovel-nosed sturgeon and long-nosed gar, which grew to over 2 m (6.5 ft) in length. Today the river can support a population of endangered Rio Grande silvery minnow only with considerable human intervention.

During the late 19th and early 20th centuries, overgrazing and logging in the headwaters resulted in the introduction of excessive sediment loads into the river system, followed by channel aggradation. Seepage from the elevated channels moved under agricultural fields and raised the water table, in many cases to that higher than the land surface. Evaporation of this water produced extensive salinization, forcing abandonment of agriculture. This problem was eventually resolved by drain and canal construction under the new Middle Rio Grande Conservation District in the 1930s.

Today, even the greatly diminished channel of the Rio Grande is seldom full. In the past 25 years, annual flows have steadily decreased compared with the second half of the 20th century. This decline can, with a fairly high degree of certainty, be attributed to increased temperature, and to a lesser degree, decreased snowfall, caused by anthropogenic global warming (Dunbar et al., 2022). Hydrologic modeling indicates likely continued decreases, amounting to 3% to 5% per decade. The Rio Grande is the principal water supply for the city of Albuquerque and for irrigated agriculture in the valley, so the cumulative negative effects of this decline will present a severe challenge for the economic future and quality of life in the region.

RIO GRANDE TERRACE STRATIGRAPHY AND VALLEY INCISION

The modern Rio Grande occupies a relatively narrow inner valley incised into axial-fluvial deposits of the upper Santa Fe Group. Incision began shortly after ~781 ka and produced a sequence of inset fluvial terraces preserved along the margins of the broader Rio Grande valley (Figs. 3.03 and 3.05; Connell et al., 2007). These deposits record episodic cut-and-fill behavior driven by changes in discharge, sediment supply, and base level.

Five inset terrace levels are recognized between San Felipe Pueblo and Los Lunas, ranging from the high, discontinuous Lomatas Negras Formation to the modern inner valley (Los Padillas Formation). These terraces form a stepped suite of valley-border landforms that record former river positions during

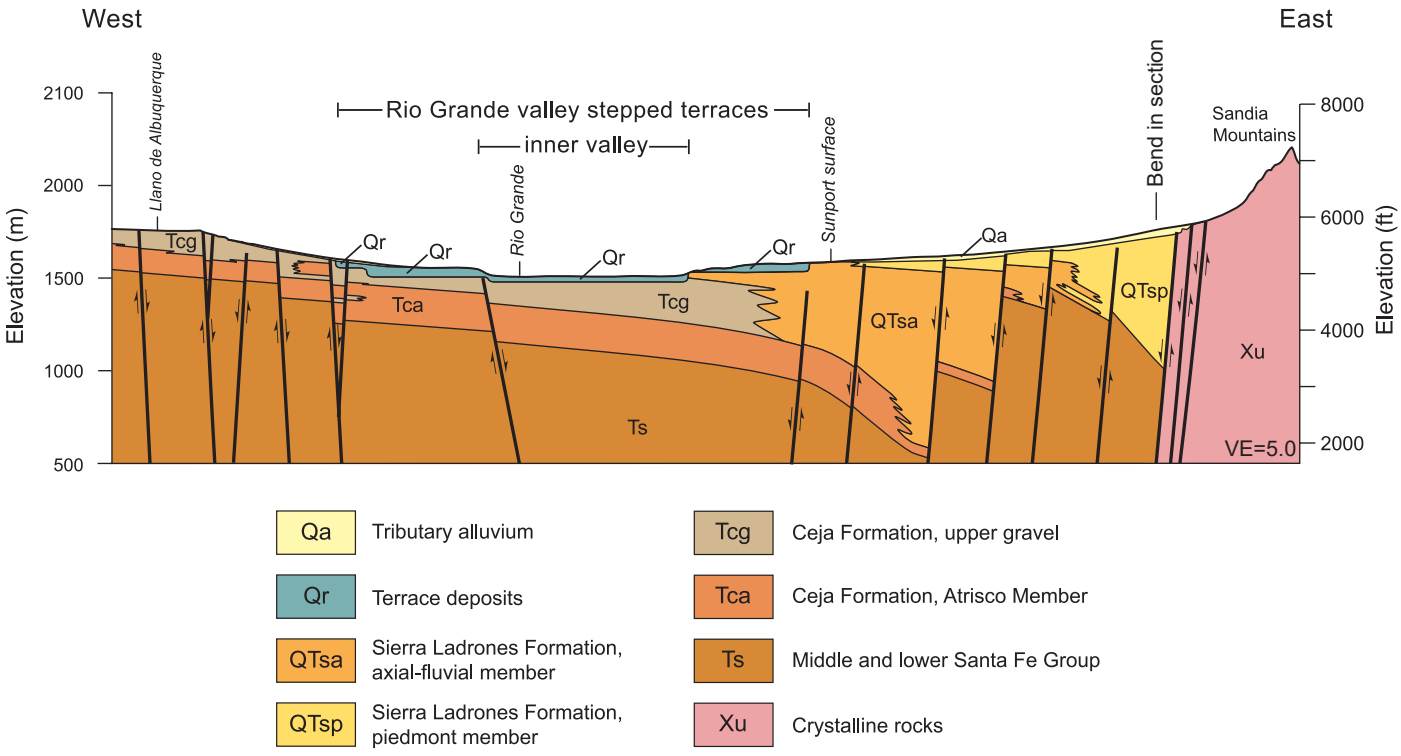


FIGURE 3.04. Simplified cross section of the Albuquerque area illustrating the difference between the stepped terraces and fill of the Rio Grande valley and subjacent basin fill of the Santa Fe Group aquifer system (from Connell et al., 2007). Note the faulted half-graben structure with tilted thick basin fill on hanging-wall blocks. This vertically exaggerated diagram (VE = 5) and is simplified from a cross section with well control by Connell (2008b). Location of the 46-km (28.6-mi)-long cross section is on Figure 3.03.

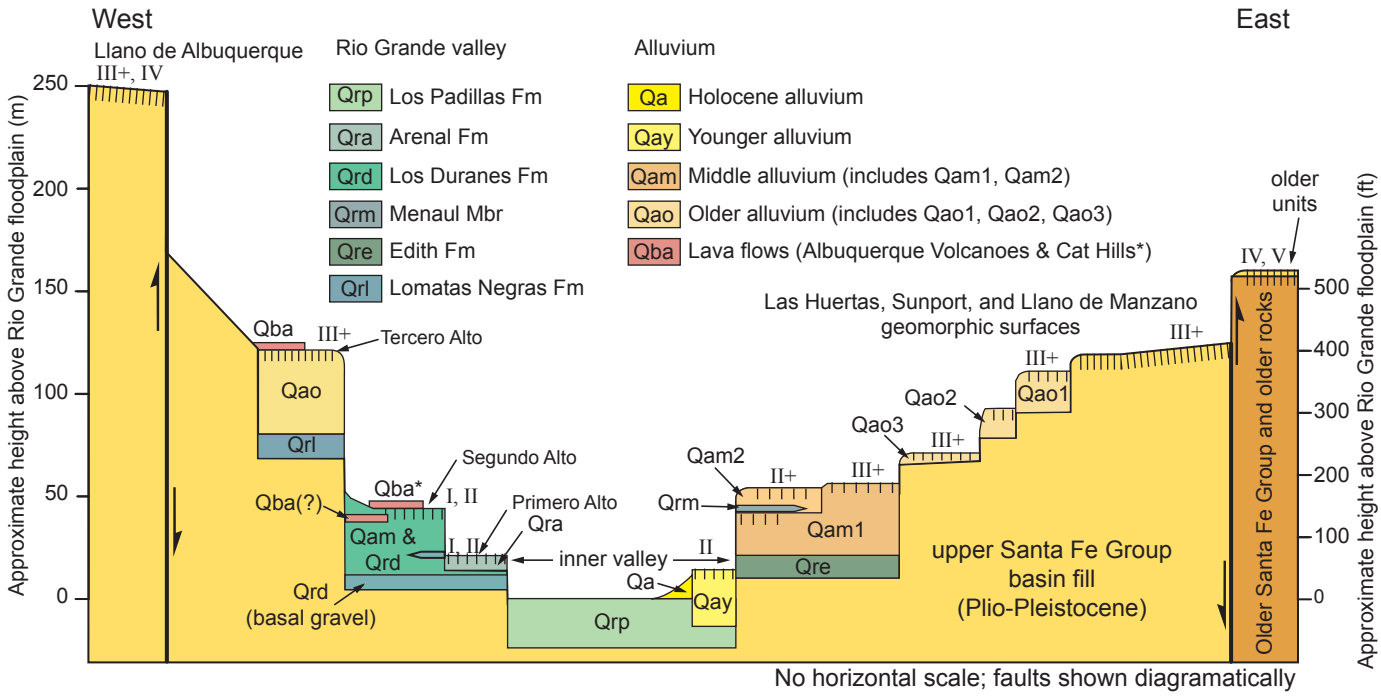


FIGURE 3.05. Schematic cross section across Rio Grande valley and adjacent piedmont and Llano de Albuquerque, illustrating landscape position and relative cross-cutting relationships among mapped Quaternary alluvial and fluvial lithologic units associated with the ancestral Rio Grande and flanking alluvial deposits (Connell et al., 2007).

progressive incision into upper Santa Fe Group basin fill (Figs. 3.04 and 3.05). Each terrace consists of a constructional tread (the former floodplain surface), a riser cut during subsequent incision, and an underlying body of terrace alluvium bounded below by a basal strath eroded into older deposits (Figs. 3.06 and 3.07). In the Albuquerque area, two of the lowest terrace levels were named Primero and Segundo Alto (i.e., first and second terrace levels) respectively in regard to their relative height above the modern floodplain (e.g., Lambert, 1968).

Terrace treads are generally narrow and discontinuous, especially on older levels, reflecting later erosion, burial by tributary alluvium, and stripping during younger cut-and-fill episodes (e.g., Figs. 3.06–3.08). Terrace deposits have a laterally extensive gravelly base overlain by finer sand, silt, and mud. Older terraces are more fragmentary and commonly mantled or buried by valley-border alluvium, whereas younger terraces preserve better-defined treads and risers. The terrace tread of the Los Duranes Formation (Segundo Alto) is approximately 6 km (3.7 mi) wide and locally inset by the Arenal Formation (Primero Alto; Fig. 3.08). A schematic cross section of the Rio Grande valley and its inner valley along Moñtano Boulevard (Fig. 3.07), approximately 9 km (5.6 mi) north of West Bluff Park, highlights hydrostratigraphic relationships of the inner Rio Grande valley, flanking river terraces, and groundwater monitoring wells (Fig. 3.07).

Mapping and correlation of terraces rely on inset relationships, soil-profile development, and independent age control from volcanic deposits. Connell et al. (2007) formalized a lithostratigraphic succession of inset river-terrace units—including the Lomatas Negras, Edith, Los Duranes (and Menaul Member), Arenal, and Los Padillas Formations—between San

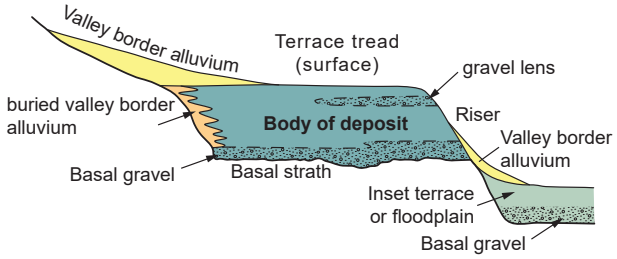


FIGURE 3.06. Schematic cross section of a terrace and underlying deposits (from Connell et al., 2007). See Figure 3.07 for an example of internal lithologic variability in the inner valley fill of Rio Grande (Los Padillas Formation).

Felipe Pueblo and Los Lunas, New Mexico (Figs. 3.03 and 3.05). A key age constraint is a fluvially recycled volcanic ash within the Lomatas Negras Formation. This ash has been correlated to the Lava Creek B tephra in the Yellowstone National Park area, located more than 1,000 km (620 mi) to the northwest. The presence of the Lava Creek B ash provides an age for that unit as well as a minimum age for the onset of valley incision (Connell et al., 2007).

Biostratigraphically significant fossils from the Edith Formation are mammalian fossils recovered from gravel pits in the greater Albuquerque area, principally the Albuquerque Gravel Products Quarry, which was located near the interchange between I-40 and I-25. These fossils are typical of the Rancholabrean Land Mammal Age and include ground sloth (*Paramylodon harlani*), bear (*Arctodus simus*), tapir (*Tapirus merriami*), horse (*Equus occidentalis*), camel (*Camelops hesternus*, *Hemiauchenia macrocephalus*), deer (*Odocoileus* sp.), bison (*Bison* sp.), mammoth (*Mammuthus columbi*), and

mastodon (*Mammut americanum*; Lucas and Logan, 1985; Lucas et al., 1988; Morgan and Lucas, 2000). Most of these mammals were large herbivores that browsed in the Pleistocene Rio Grande bosque, which, as far back as about 1.2 Ma, supported vegetation very similar to that of the present-day bosque (Knight et al., 1986), or grazed in adjacent parklands and savannas. They are, nevertheless, not particularly precise age indicators because the Rancholabrean Land Mammal Age covers the time between about 250 ka and 10 ka.

The Los Duranes Formation is bracketed by basaltic lava flows with ages of about 211–100 ka and may be correlative to the Edith Formation (Morgan and Harris, 2015). Los Duranes Formation deposits in the Martinez Gravel Pit in Bernalillo, Sandoval County, produced an incomplete skull of the giant *Bison latifrons* (Smartt et al., 1991). This may be one of the oldest, well-dated records for the appearance of *Bison* in the southwestern United States.

Terraces are commonly unpaired across the valley, reflecting asymmetric preservation and lateral migration of the river within a structurally segmented half-graben. Terrace treads tend to be sandy and vulnerable to erosion. Tributary drainages and eolian processes can deliver sediment to the incised river terrace and aggrade notable thicknesses of sand. Therefore, correlation by height alone is generally not reliable. Terrace identification relies on relative inset relations, basal strath elevation, deposit thickness, and soil-morphologic development rather than simple elevation matching, which can be challenging because of variable quality of exposures.

Terrace development reflects episodic alternation between incision and aggradation driven by changes in stream power, sediment supply, and climate (e.g., Bull, 1991). Incision events cut new straths into Ceja and Sierra Ladrones Formation basin fill, lowering base level and creating terrace risers (Figs. 3.03, 3.05, and 3.08). These episodes were followed by partial valley backfilling during periods of reduced transport capacity or increased sediment supply, forming constructional treads and associated terrace deposits.

Aggradational phases commonly begin with high-energy gravel deposition, interpreted as intervals of increased discharge and competence, followed by upward-fining successions that record waning flow energy, floodplain expansion, and enhanced fine-sediment storage. Thicker successions (e.g., the Los Duranes and Los Padillas Formations) may reflect more sustained sediment input, whereas thinner, single fining-upward packages (e.g., the Edith and Arenal Formations) represent shorter-duration responses to climatic or hydrologic shifts.

Complementary but conceptually different syntheses of these deposits were presented by Connell et al. (2007) and Cole et al. (2007), each emphasizing distinct stratigraphic frameworks, correlation strategies, and age controls. Connell et al. (2007) emphasized geomorphic-sedimentologic analysis and lithostratigraphic formalization of inset terrace deposits between San Felipe Pueblo and Los Lunas. Building on previous work by Lambert (1968), Connell et al. (2007) formalized a succession of discrete inset fluvial units named the Lomatas Negras, Edith, Los Duranes (and Menaul Member), Arenal, and Los Padillas Formations (Figs. 3.05 and 3.08). These units were defined by mappable geometry, basal strath heights, facies assemblages, and degree of soil development. Their framework highlighted the importance of cut-and-fill episodes, and variable preservation of terrace treads. A key contribution was the identification of fluvially recycled tephra of the ~631 ka (Matthews et al., 2015) Lava Creek B tephra within the Lomatas Negras Formation, providing a minimum age for the onset of Rio Grande valley incision in the Albuquerque area. Connell et al. (2007) interpreted terrace formation as the product of punctuated changes in stream power and sediment supply, largely driven by climatic variability superimposed on long-term tectonic subsidence. The Albuquerque area terrace chronology of Connell et al. (2007) correlates reasonably well to a suite of well-dated terraces in the Socorro area, less than 100 km (62

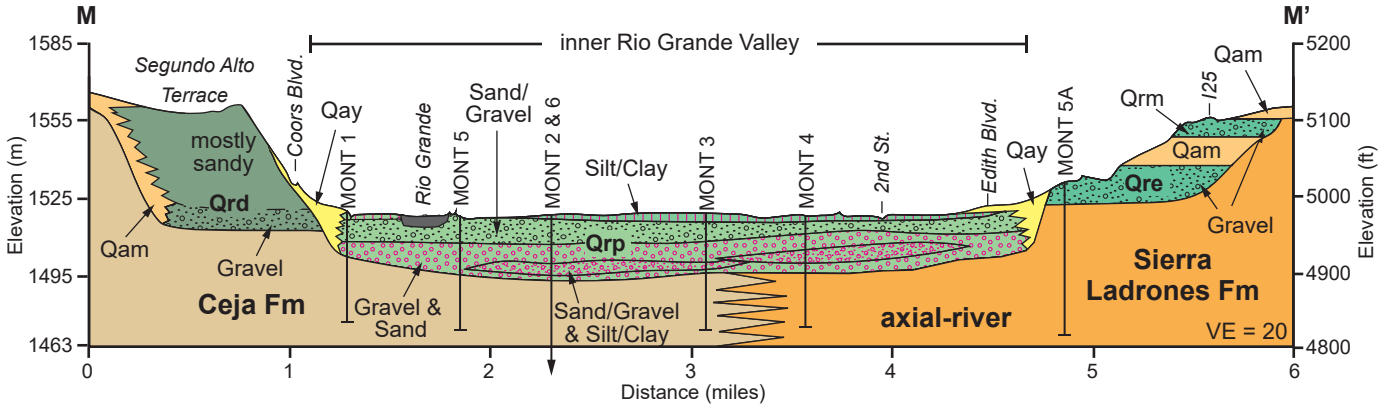


FIGURE 3.07. Schematic geologic cross section of the Rio Grande valley along Montaño Boulevard, between San Ildefonso Drive and Carlisle Boulevard (Raymond et al., 2010). On this vertically exaggerated cross section (VE = 20), unit Qrp refers to river floodplain and channel deposits of the Los Padillas Formation (Holocene/latest Pleistocene). Unit Qay denotes younger alluvium and associated eolian sediments of tributary-arroyo systems that interfinger with unit Qrp along the borders of the inner valley of the Rio Grande. Unit Qrd refers to river-terrace deposits of the late–middle Pleistocene Los Duranes Formation, showing a basal gravel zone that is below the modern floodplain. Unit Qre refers to terrace deposits, including gravel of the middle Pleistocene Edith Formation and Menaul Member. Unit Qam refers to intermediate alluvium and associated eolian sediments of tributary-arroyo systems graded to the Los Duranes Formation and interfingers with and overlies the Edith Formation and Menaul Member.

mi) downstream (Sion et al., 2020).

Cole et al. (2007) focused on numerical age control and regional correlation of terrace-fill deposits using optically stimulated luminescence (OSL) and thermoluminescence (TL) dating at limited locations. They correlated expanded on Lambert's (1968) terrace-level chronology to include four terrace surfaces: Primero, Segundo, Tercero, and Cuarto Alto (i.e., first, second, third, and fourth terrace levels, respectively). These terrace surfaces were correlated primarily by height above the modern floodplain and downvalley continuity of projected terrace treads (e.g., Lambert, 1968). Cole et al. (2007) proposed terrace formation during aggradational episodes that correspond broadly to glacial-interglacial climate cycles. Primero Alto aggradation occurred during Marine Isotope Stage 3 (~47–40 ka), and Segundo Alto during early Marine Isotope Stage 5 (~98–90 ka). Ages of deposition of older terraces are constrained by an occurrence of the Lava Creek B tephra and Bandelier Tuff as described in Connell et al. (2007). Cole et al. (2007) contended that despite lithologic variability and local source contributions, these largely unpaired terrace fills can be reliably correlated across the valley as unconformity bounded (allostratigraphic) units.

Principal differences between these two interpretations generally relate to stratigraphic nomenclature and correlation criteria. A related debate centers on whether terraces are best interpreted as multiple short-lived cut-and-fill events (Connell et al., 2007) or as prolonged aggradational phases culminating in regionally correlative terraces (Cole et al., 2007). Connell et al. (2007) advocated lithostratigraphic definitions tied to facies architecture, soil-profile development, and mapped inset relationships, cautioning against sole reliance on terrace height because of differential preservation, erosion, and fault-related tilting. Cole et al. (2007) viewed many of the named lithostratigraphic units (e.g., Edith, Los Duranes, and Menaul) as lithologically heterogeneous components of larger allostratigraphic terrace-fill successions.

Despite these different conceptual models, both studies converge on key conclusions: (1) the Rio Grande has undergone repeated incision punctuated by aggradation; (2) terrace formation is linked to climate-driven variations in discharge and sediment supply; and (3) volcanic tephra and basalt flows provide critical, independent age constraints. Together, these studies form a framework for interpreting Rio Grande valley evolution and underscore the importance of integrating geomorphology, sedimentology, soil stratigraphy, and geochronology to interpret long-term fluvial histories in the Rio Grande rift.

HYDROGEOLOGY OF THE SANTA FE GROUP AQUIFER SYSTEM

The Santa Fe Group forms the principal regional aquifer system of the Middle Rio Grande Basin, including the Albuquerque Basin, and consists of structurally segmented and lithologically heterogeneous assemblages of primarily Neogene syn-rift basin fill related to the tectonic and depositional evolution of the Rio Grande rift (e.g., Hawley and Kernodle, 1999; Connell, 2004). Hydrogeologically, the Santa Fe Group is not a single, laterally continuous aquifer but a composite system of variably connected fluvial sand and gravel bodies interbedded with laterally discontinuous to regionally extensive fine-grained deposits that exert controls on groundwater flow, vertical connectivity, and water quality (Fig. 3.04). The distribution and hydraulic properties of permeable intervals are



FIGURE 3.08. View to south of Arenal Formation (Primero Alto terrace surface), which is erosionally inset against the Los Duranes Formation just south of the I-40 bridge over the Rio Grande. Volcanic features on the southern skyline include (from left to right), Tomé Hill, Isleta Volcano, Los Lunas Volcano (Cerros de los Lunas), and Wind Mesa. Ladron Mountains are in the far distance to the right.

strongly influenced stream-power variations associated with particular depositional environments (e.g., proximal-to-distal piedmont, floodplain, and former positions of the ancestral Rio Grande). In turn, these depositional environments and catchments are controlled by rift-related subsidence patterns, basin segmentation, syntectonic sedimentation, paleoclimate variations, and evolving depositional systems (Connell, 2004; Connell et al., 2013; Koning et al., 2019).

In the Albuquerque Basin, the Santa Fe Group thickens from a few hundred meters near basin margins (near Day 2 stops) to more than 4 km (2.5 mi) in the basin depocenter (Lozinsky, 1994; Connell, 2004); however, groundwater development is largely restricted to the upper ~600 m (~1,970 ft) of basin fill because of declining permeability and increasingly degraded water quality at greater depths (e.g., Hawley and Haase, 1992). Groundwater flow is anisotropic, meaning it flows more easily horizontally than vertically. This is due to the presence of laterally extensive fluvial sand and gravel bodies that are interbedded with low-permeability floodplain, local playa-lake, and paleosol-bearing deposits (Kernodle et al., 1995).

Hydrostratigraphic refinement of the Santa Fe Group follows the lithostratigraphic framework of Connell and coworkers, who subdivided the basin fill into the Arroyo Ojito, Ceja, and Sierra Ladrones Formations (Connell, 2004, 2008a; Koning et al., 1999). This lithostratigraphic framework improves correspondence among depositional environments, hydraulic properties, and groundwater chemistry relative to earlier lower–middle–upper subgroup nomenclature.

Plummer et al. (2024) conducted an extensive study of groundwater chemistry of the Santa Fe Group and Los Padillas Formation. Lower Santa Fe Group deposits, including the Zia and Cerro Conejo Formations, are broadly correlative with the lower Santa Fe Group and parts of the middle Santa Fe Group. These units locally form productive aquifers along the northwestern basin margin but commonly yield groundwater with moderate to high total dissolved solids (TDS) and chemically evolved compositions reflecting long residence times and extensive water–rock interaction. A notable exception is in the Cerro Conejo Formation, near Rio Rancho, where the upper 50–100 m (160–330 ft) of this middle Santa Fe Group aquifer contains laterally extensive sandstone that may be highly permeable, based on limited aquifer tests (Koning et al., 2026a, 2026b).

The Arroyo Ojito Formation corresponds to the middle Santa Fe Group and records deposition in internally drained to poorly integrated basins dominated by alluvial, eolian, and playa-lake depositional systems. Although the unit exhibits an overall upward-coarsening trend, abundant clay-rich and paleosol-bearing intervals reduce vertical hydraulic connectivity and result in generally lower hydraulic conductivity than in overlying units (e.g., Koning et al., 2026a, 2026b). Groundwater in the Arroyo Ojito Formation is typically older and more chemically evolved and may be locally enriched in arsenic, fluoride, and other trace elements under reduced conditions and prolonged water–sediment interaction (e.g., Hawley and Haase, 1992; Plummer et al., 2004). Consequently, deposits of the Arroyo Ojito Formation represent a somewhat lower-quality aquifer system and semiconfining hydrostratigraphic subunits beneath western Albuquerque and Rio Rancho.

The Ceja and Sierra Ladrones Formations make up the upper Santa Fe Group, and mark basin integration and correspond with the development of the ancestral Rio Grande and tributary fluvial systems during late Miocene and early Pliocene time (Connell, 2004; Koning et al., 2019). The Ceja Formation consists predominantly of sand, gravelly sand, and conglomerate interbedded with paleosols and subordinate fine-grained deposits. Much of the Ceja Formation lies within the vadose zone beneath the Llano de Albuquerque and West Mesa; however, thicker saturated intervals occur basinward where the unit thickens structurally. Groundwater is generally moderately mineralized, but fault-controlled facies changes and paleosol horizons contribute to aquifer compartmentalization and spatial variability in water chemistry (Plummer et al., 2004).

The Sierra Ladrones Formation forms the uppermost part of the Santa Fe Group across much of eastern Albuquerque and records establishment of a fully integrated ancestral Rio Grande fluvial system (Connell et al., 2005). Laterally extensive axial-river sand and gravel deposits are highly permeable and yield the highest transmissivity values in the regional aquifer system, forming the core of modern municipal well fields. Groundwater in the axial-river facies has relatively low TDS near the Rio Grande and becomes progressively more chemically mature away from the river and with depth due to longer residence times and mixing with older basin-fill waters (Plummer et al., 2004). Piedmont facies consist of coarse basin-margin deposits; despite the coarser grain size, permeability is commonly reduced by fine-grained matrix and carbonate cementation, resulting in heterogeneous hydraulic behavior and greater geochemical variability. These deposits primarily function as zones of mountain-front recharge rather than laterally extensive aquifers.

Inset Pleistocene and Holocene alluvium along the modern Rio Grande valley contains the youngest and least chemically evolved groundwater in the basin. Groundwaters analyzed from these deposits reflect active recharge from river leakage, irrigation return flow, and local runoff. However, the groundwaters in these aquifers are also the most susceptible to anthropogenic impacts, including elevated nitrate and localized increases in dissolved solids (Plummer et al., 2004).

Groundwater Monitoring and Aquifer Recharge

The U.S. Geological Survey, in cooperation with Albuquerque-Bernalillo County Water Authority (Water Authority), drilled and installed a nest of piezometers on West Bluff Park in 1996 (Fig. 3.09). At this site, two wells were drilled to install 6 piezometers to monitor groundwater levels at multiple depths at a single location. The deepest nest was drilled to a depth of 335 m (1,100 ft) below ground surface. The purpose of these piezometers was to measure and monitor vertical hydraulic gradients in the regional Santa Fe Group aquifer system (Donohoe and Moore, 2003). The installation consists of three deeper piezometers in one well, and three shallower piezometers in the other (Fig. 3.09). Each piezometer was screened over a 1.5-m

(5-ft)-long interval to isolate discrete depth zones.

The West Bluff nests provide colocated hydraulic head measurements that allow separation of basin-scale temporal signals (driven by pumping, recharge, and management-driven changes) from depth-dependent responses related to vertical anisotropy, semiconfining intervals, and vertical leakage between hydrostratigraphic zones in the regional Santa Fe Group aquifer system. Based on initial water level measurements, the shallow nest of piezometers shows little difference in water-level elevation with depth, but the deeper nest shows a trend of increasing hydraulic head with depth, indicating vertical flow. The aquifer in the shallow zone is probably influenced by the Rio Grande. The slight upward gradient in the deeper zones probably indicates deeper flow paths and a less direct connection to the Rio Grande.

The Rio Grande locally provides natural recharge into the upper Santa Fe Group. Humans can also engineer recharge using water diverted from the river. Since 2008, Water Authority has been drawing surface water from the Rio Grande. Approximately 10 km (6 mi) upstream (north) of West Bluff Park, near Alameda Boulevard, surface water is diverted from the Rio Grande and conveyed approximately 6 km (<4 mi) to the southeast to the San Juan-Chama Drinking Water Treatment Plant. In 2018–2019, Water Authority funded a study to identify potential areas to recharge the Santa Fe Group aquifer using Rio Grande water (Koning et al., 2019, 2026e). Two recharge methods were considered (1) shallow-recharge, where water is spread on the surface and allowed to infiltrate into the ground; and (2) deep-injection directly from wells screened in the aquifer. A map showing favorable areas for the shallow recharge is shown in Figure 3.10. An area interpreted to be favorable to shallow recharge extends north of Central Avenue to the vicinity of Paseo del Norte Boulevard, and between the Rio Grande floodplain and Eubank Boulevard. A major factor choosing this area is the subsurface geology. Specifically, thick deposits of sandy sediment in this area were deposited by the ancestral Rio Grande during the past several million years (i.e., the axial-fluvial facies in the Sierra Ladrones Formation).

End of Stop 1

REZERO ODOMETER before leaving STOP 1.

0.0 Drive about 45 m (150 ft) north on Vista Grande Drive NW **before turning left (west) onto Ian Avenue NW.** *0.1*

0.1 **Turn right (north) onto Alamogordo Road NW.** *0.1*

0.2 **Turn left (west) onto Ouray Road NW.** *0.2*

0.4 Move to left lane. *0.1*

0.5 **Turn left onto I-40 on-ramp.** *0.2*

0.7 **Use the right two lanes to merge onto westbound I-40 towards Gallup, New Mexico**. *0.5*

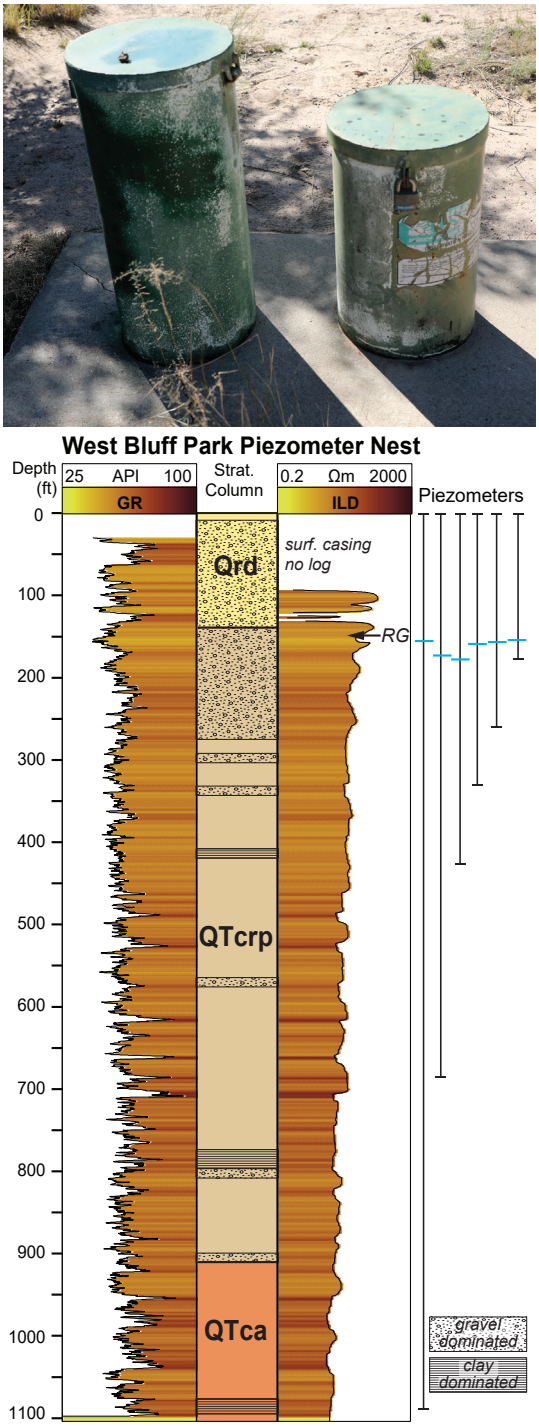


FIGURE 3.09. Photograph of West Bluff Park piezometer nests (top; USGS Well ID 350638106413701–06) and well log (bottom). Lithologic units include the Los Duranes Formation (Qrd), Rio Puerco Member (QTcrp), and Atrisco Member (QTca) of the Ceja Formation. Gravel and clay-dominated intervals are shown by lithologic symbols. The RG label and arrow denote the projected depth of the Rio Grande floodplain. Three piezometers were installed at each well. Each as a screened interval of 1.5 m (5 ft). The top of screen for the deep piezometers are at 132, 210, and 334 m (433, 689, and 1,096 ft, respectively) below land surface. The top of screen for the shallow piezometers are at 53, 77, and 100 m (174, 253, and 328 ft, respectively) below land surface. The short blue lines denote the depth to water in each piezometer just after completion of the wells. Overall, the Ceja Formation coarsens upward as shown by the natural gamma ray (GR) and resistivity (ILD) logs.

1.2 Drive across a low-relief surface, which is the depositional-terrace tread of the Segundo Alto terrace surface mapped by Lambert (1968), which is the top of the Los Duranes Formation. Lava flows of the Albuquerque Volcanoes form a prominent linear scarp at 2:00 (Fig. 3.11). Landslides that developed on this escarpment are described in Haneberg and Connell (2026). *0.8*

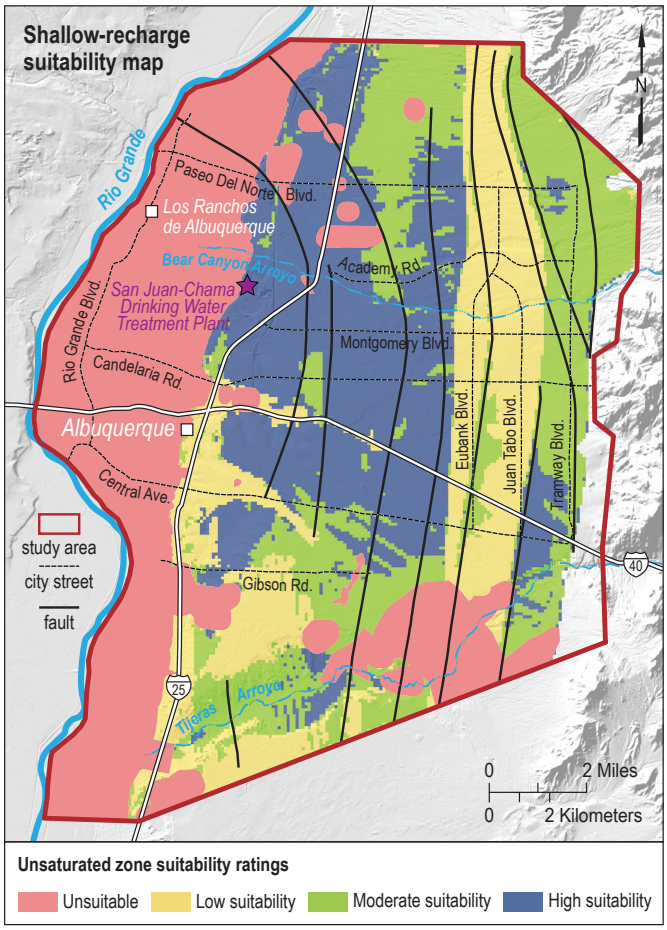


FIGURE 3.10. Map illustrating suitability regions for shallow-based recharge to the Santa Fe Group aquifer underlying Albuquerque, east of the Rio Grande (from Koning et al., 2019, 2026e).

2.0 Pass off-ramp for Unser Boulevard (Exit 154) and continue west on I-40. *0.8*

2.8 Ascend gently sloping valley-margin fans that have prograded across the western tread of the Segundo Alto terrace surface. *0.5*

3.3 Pass Exit 153 off-ramp for Ninety-Eighth Street and Arroyo Vista Boulevard. On the north side of the off-ramp is the location of the exploratory 98th Street well (Fig. 3.12). This well was drilled in the 1990s to 457 m (1,500 ft) in order to better understand the geochemistry of the underlying aquifer and water quality (e.g., Bartolino and Cole, 2002). Interpretation of core, drillhole cuttings, and borehole geophysical logs identified an overall coarsening-upward trend that corresponds to the Rio Puerco and Atrisco Members of the Ceja Formation (e.g., Allen et al., 1998; Connell et al., 1998; Connell, 2008b). Many of the water-supply wells beneath northeast Albuquerque are completed in aquifers above the Atrisco Member, whereas many water-supply wells west of the Rio Grande produce water above and below the Atrisco Member. Water-supply wells drawing from the Atrisco Member and lower units commonly have elevated levels of arsenic (>10 µg/L in Melis and Peery, 2017). *0.3*

3.6 Cross Ninety-Eighth Street overpass and continue west on I-40, traveling up Nine Mile Hill, which culminates at a white-rimmed mesa known as Cejita Blanca (Kelley, 1977). This white-rimmed mesa is also known as the Llano de Albuquerque (Machette, 1985). The Llano de Albuquerque commonly has 1–2 m (3–6 ft)-thick light-gray petrocalcic paleosols that exhibit Stage III to Stage III+ carbonate morphology and form the Cejita Blanca of Kelley (1977). The Llano de Albuquerque represents an abandoned relict depositional surface developed on top of the Ceja Formation (Connell, 2008a). Underneath the Llano de Albuquerque surface are gravelly sands of the Plio–Pleistocene Rio Puerco Member of the Ceja Formation (Connell, 2008b). *1.7*

5.3 Light-gray to white soil-bounded sandy wedges on right are part of a complicated set of sedimentary

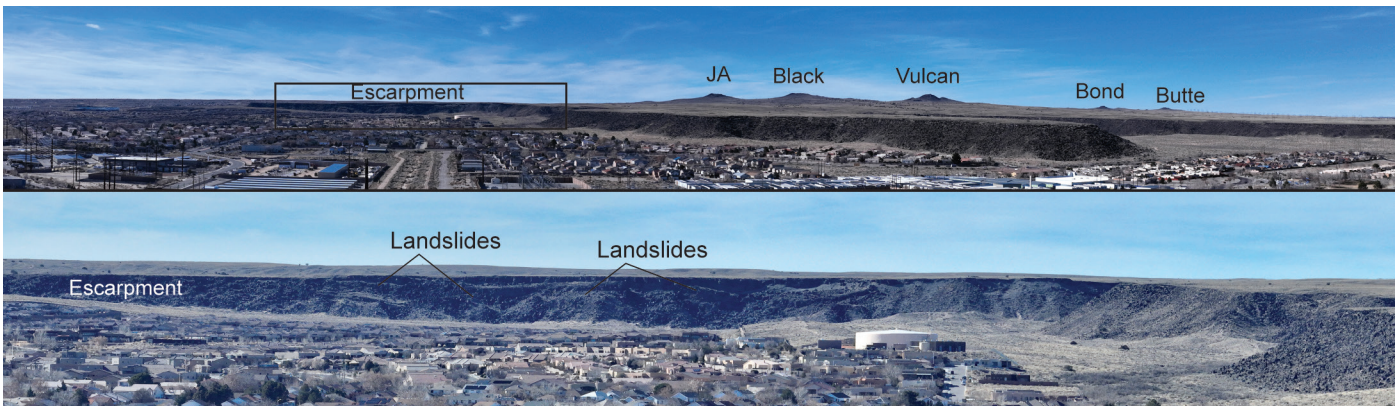


FIGURE 3.11. View to west of the Albuquerque Volcanoes and major vents (top). The black rectangle denotes part of an east-facing escarpment that was formed by lava flows from the volcanoes. Bottom: close-up view of landslide blocks along an unusually linear, south-trending face of basaltic lava flows. Landslide and the evolution of this escarpment are discussed in Haneberg and Connell (2026).

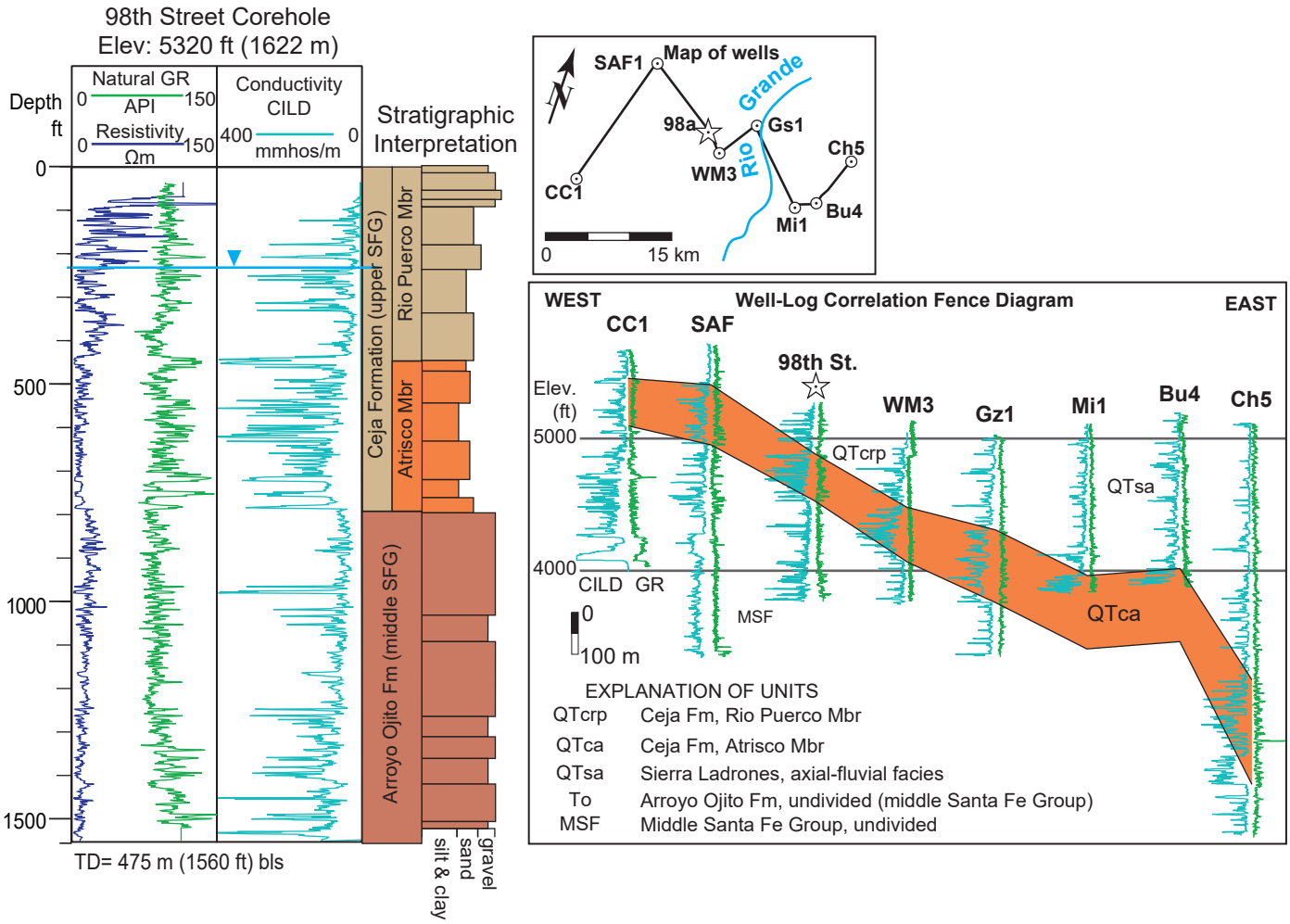


FIGURE 3.12. Borehole log information from USGS 98th Street well and well-log correlations (modified from Allen et al., 1998, and Connell et al., 1998).

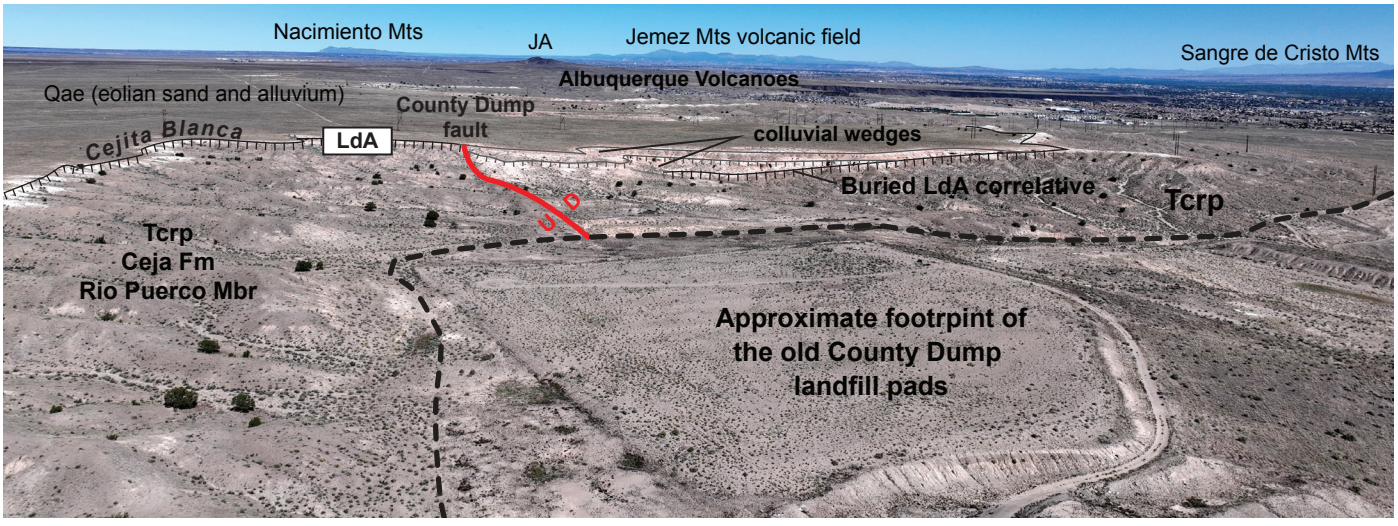


FIGURE 3.13. Colluvial wedge deposits formed along the proximal hanging wall of the County Dump fault, an intrabasinal normal fault that trends north towards the Albuquerque Volcanoes. Nacimiento, Jemez, and Sangre de Cristo Mountains frame the northern skyline. The County Dump fault offsets the Llano de Albuquerque surface (LdA), which forms the white rim of Cejita Blanca of Kelley (1977). The Llano de Albuquerque is recognized by a strongly developed petrocalcic soil with Stage III+ carbonate morphology (black hachured lines). To the right (east) is a stack of paleosols that developed proximal to the hanging wall of the County Dump fault. The lowest, strongly developed petrocalcic soils are correlated to the Llano de Albuquerque. Machette (1978) studied these exposures and developed a conceptual soil-stratigraphic model of interpreting earthquake events using soil-morphologic mapping. A prominent paleosol marker is represented by gray hachures. McCalpin et al. (2006) refined the paleoseismic chronology in a series of excavations.

wedges that formed in response to long-term movement along the County Dump fault (Fig. 3.13). Fault-bounded colluvial wedges consist of scarp-derived colluvium that accumulate at the base of a fault scarp immediately following surface rupture (see Machette, 1978). They formed syndepositionally with (or shortly after) surface rupture as eroded sediment (e.g., colluvium, alluvium, and sheetwash, slopewash, and eolian deposits) collapses from the newly formed scarp. Subsequent burial by younger deposits as discrete event horizons in natural exposures and excavations provide useful indicators of past surface-faulting events. Fault-bounded colluvial wedges can be used to constrain the timing of paleoearthquakes by examining cross-cutting relationships and dating scarp-derived colluvial deposits adjacent to the fault (McCalpin, 1996). Slip estimates derived from these features should be regarded as minimum values and interpreted cautiously because they are sensitive to post-rupture processes, sediment supply (from fault scarp or other sources, such as eolian sand), and preservation (McCalpin et al., 2006). *0.5*

5.8 County Dump fault exposed on right (north). It is recognized here by an abrupt contrast between light-gray sand on the footwall, and light-brown to pinkish pebbly sandstone on the hanging wall (Fig. 3.14). This fault zone projects north to the parking area at Stop 2. *0.2*

6.0 **Take off-ramp for Atrisco Vista Boulevard toward State Road 500 (NM 500) and west-side access to Petroglyph National Monument (Exit 149).** The trip route will rely on a geologic map of the Albuquerque Volcanoes for reference (Fig. 3.15). *0.3*

6.3 **Turn right and head northwest on Atrisco Vista Boulevard.** We are driving on a gently south-sloping, low-relief surface developed on surficial sand capping the Ceja Formation (upper Santa Fe Group). The uppermost Santa Fe Group is not exposed here, but on the west and east edge of the Llano de Albuquerque, it is gravelly and part of the Rio Puerco Member of the Ceja Formation. Overlying the top of the Rio Puerco Member contains 1–10 m (3–30 ft) of very fine- to medium-grained sand and silty clay interpreted as eolian sand sheets that were typically reworked by sheetwash processes, eolian sand dunes, and local mud-filled depressions (Thompson et al., 2009).

Relief on the Llano de Albuquerque surface ranges from about 3 m to over 15 m (10 to 50 ft). This relief is interpreted to represent local sand sheets, eolian sand dunes, and local mud-filled depressions and buried faults, some of which have been identified using aeromagnetic datasets (Grauch et al., 2001; Connell, 2008a). *2.7*

9.0 Pliocene volcanic center of Mount Taylor at 9:00. The Sierra Nacimiento frames skyline at 11:00. The Jemez Mountains are 12:00 and 1:00. The Sangre de Cristo Mountains form the distance skyline between 1:00 and 2:00. The Sandia Mountains are between 2:00 and 4:00. *1.0*

10.0 View ahead of the southern cones (from north to south Black, Vulcan, and JA) of the Albuquerque Volcanoes. *1.1*

11.1 **Turn right onto Petroglyph National Monument Access Road to the Five Volcano Trailhead parking lot.** *0.3*

11.4 Park vehicle.

Waypoint 3.03 [N35.1306°, W106.7801°]

STOP 2: Five Volcanoes Trailhead.

INTRODUCTION

The Albuquerque Volcanoes are part of a Pleistocene basaltic volcanic field on the western edge of Albuquerque, where aligned vents, cinder cones, and lava flows form a north-trending

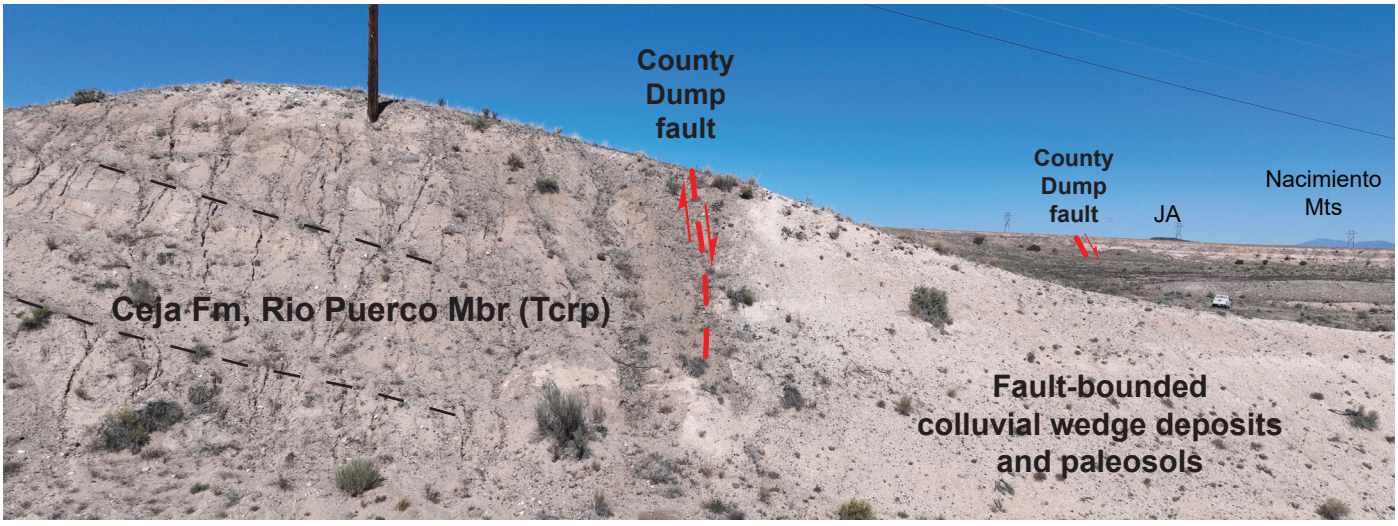


FIGURE 3.14. View to north of County Dump fault along access road on north side of I-40. Down-dropped (hanging-wall) side is on the right side of the photograph. In the distance to the right are the stacked paleosols of the colluvial wedge described in Figure 3.13.

volcanic ridge along the eastern margin of the Llano de Albuquerque (Fig. 3.15). Kelley and Kudo (1978) identified the field as part of the broader basaltic volcanism of the Albuquerque Basin and emphasized its petrology, fissure control, and relationship to basin structure. Recent mapping by Thompson et al. (2020a, 2020b) refined the volcanic stratigraphy and showed

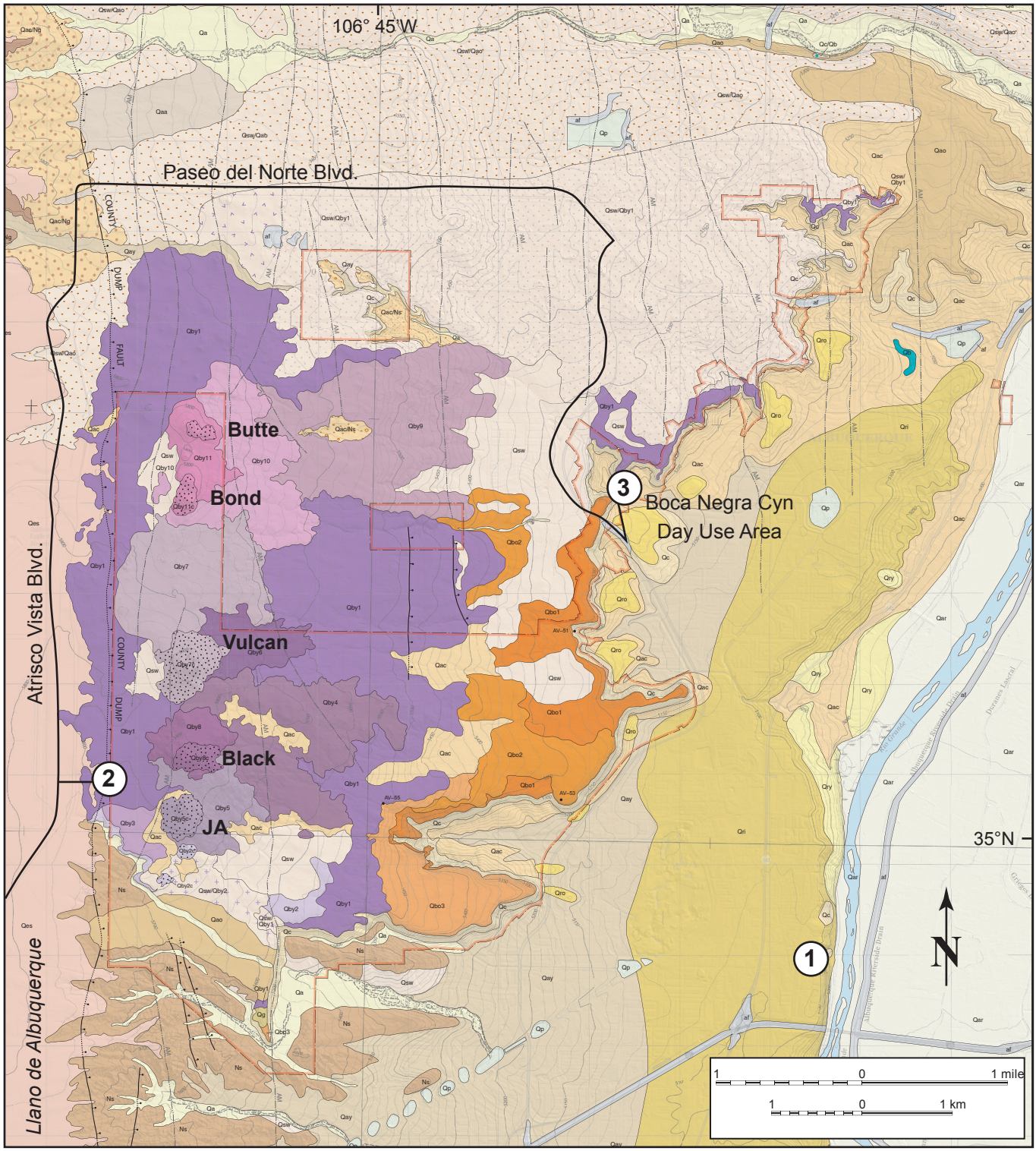


FIGURE 3.15. Generalized geologic map of the Albuquerque Volcanoes (modified from Thompson et al., 2020a). Day 3 stops are shown in white circles. Refer to Thompson et al. (2020a) for explanation of map units.

that the preserved vents and basin-filling flows are closely associated with extensional faults, reinforcing interpretations that magma ascent and vent alignment were influenced by rift-related structures.

The Albuquerque Volcanoes cover an area of 50–60 km^2 (19 mi^2) and have an estimated volume of 0.2–0.5 km^3 (0.05–0.12 mi^3). Uncertainty in the areal extent results from differing assumptions about the extents of lava flows, particularly on the north end where thick sediment and vegetation obscure flow margins. Uncertainty in the volume of the volcanic field arises from several factors. First, the thickness of lava sheets varies, especially near the fissure where the terrain is built up. Second, variations in original relief increase ambiguity. Lastly, the original extent of the lava sheets is not clear due to incision, back-wasting of flow margins, and the possibility that some flows extended into an ancestral Rio Grande paleovalley.

We are in Petroglyph National Monument. Collecting is prohibited, so leave your rock hammer in the car and stay on marked trails. At this stop, we will discuss the volcanic history of the central Albuquerque Basin. Following this overview, we will hike towards Black Volcano (Fig. 3.16 and 3.17).

ALBUQUERQUE VOLCANOES PHYSICAL VOLCANOLOGY

At this stop, we ascend Black Volcano and discuss the structure and development of a basaltic eruption from a long fissure (Figs. 3.17–3.19). The Albuquerque Volcanoes represent the latest eruption in the central Rio Grande rift. Because the lava flows of the Albuquerque Volcanoes record a middle Pleistocene geomagnetic anomaly, considerable effort has been made to accurately date the eruptions of the Albuquerque Volcanoes. Current age determinations range from 156 to 218 ka (Zimmerer, 2024). This age range comes from a $^{238}U/^{230}Th$ date of 156 ± 29 ka (Peate et al., 1995), and $^{40}Ar/^{39}Ar$ dates of 211 ± 13 ka (Singer et al., 2008). This age range fits with the general state of morphologic preservation of smaller-scale volcanic features in similarly dated volcanic areas in New Mexico.

Compositionally, the eruption was somewhat unusual for the southwestern United States in general and the Rio Grande rift in particular. Rocks are composed of olivine tholeiite with 47–52 wt% SiO_2 and less than 4 wt% K_2O and Na_2O (Kelley and Kudo, 1978; Baldridge, 1979; Thompson et al., 2020a, 2020b), rather than more alkaline compositions recognized in many volcanic fields throughout New Mexico and the Rio Grande rift. A notable exception is the McCartys basaltic lava flow, about 90 km west, near Grants, New Mexico.

Basaltic rock specimens exhibit a dark groundmass of plagioclase, olivine, and augite with prominent small (<1-mm long) olivine and plagioclase phenocrysts. Uncommonly, there are xenoliths of upper crustal materials, mostly of sandstone, that can be several centimeters in diameter and partially melted.

Earlier activity produced extensive lava flows. Volcanic cones were built up in the latter phase of the eruptions. The principal cones are accumulations of scoria, agglutinate, spatter, and breccias (locally altered by fumarole activity) interlayered with thin basaltic sheet flows and spill-over flows that form radially oriented digitate (finger-like) lobes 1–4 m (3–13 ft) wide and several hundred meters in length. These give way farther out to extensive sheets of pāhoehoe lava flows with well-developed tumuli and numerous lava channels, particularly near the distal edges. The lavas are generally less than 3 m (10 ft) in thickness and flowed down the regional gradient and paleodrainages toward the Rio Grande as channelized flows and compound pāhoehoe flow stacks.

Inflation, a characteristic of most pāhoehoe lava sheets in New Mexico (e.g., Crumpler et al., 2013), is not generally present; however, inflation structures can be locally observed, except in a few small terminal lava tongues and tumuli where small break-outs have formed lava gutters and related features of lava emplacement, and near terminal ends where the lava thickens. An example of the latter is at the Boca Negra Canyon area of Petroglyph National Monument, where unusual vesicle cylinders formed within inflated interiors of flow sheets. Vesicle cylinders are discussed at Stop 3 (Goff, 2026). Where exposed along escarpments and in roadcuts, both multiple elliptical compound flows and inflated massive basalt sections are present. Throughout this volcanic field, exposed sections also preserve the characteristic vertical zonation of vesicles abundance first noted by Aubele et al. (1988) and now recognized in pāhoehoe flows globally (Cashman and Kauahikaua, 1997; Self et al., 1998) and on other planets. The vertical zonation consists of downward increasing vesicle size and upward increasing vesicle density reflecting the competition between vesicle growth and the interiorward advance of the solidification front toward the interior of a flow as the lavas cooled.

Eruptions took place from a pair of north-trending fissures. Collectively, the pair is of somewhat unusual length (between 4.5 and 6.0 km [2.8 and 3.7 mi]) compared with most Quaternary eruptive fissures in the Southwest. At most monogenetic basaltic vents, the initiating fissure is commonly less than a few hundred meters long and generally obscured by the resulting scoria cone built during the subsequent eruption. The Albuquerque Volcanoes fissure is more akin to the long fissures that are common in Iceland and Hawaii (Fig. 3.20).

The arrangement of the five volcanoes here reflects a typical evolution along a long fissure. Assuming that this fissure behaved like a modern fissure, optically dense fire fountains



FIGURE 3.16. Photograph of Vulcan (left), Black (middle), and JA (right) cones of the Albuquerque Volcanoes.

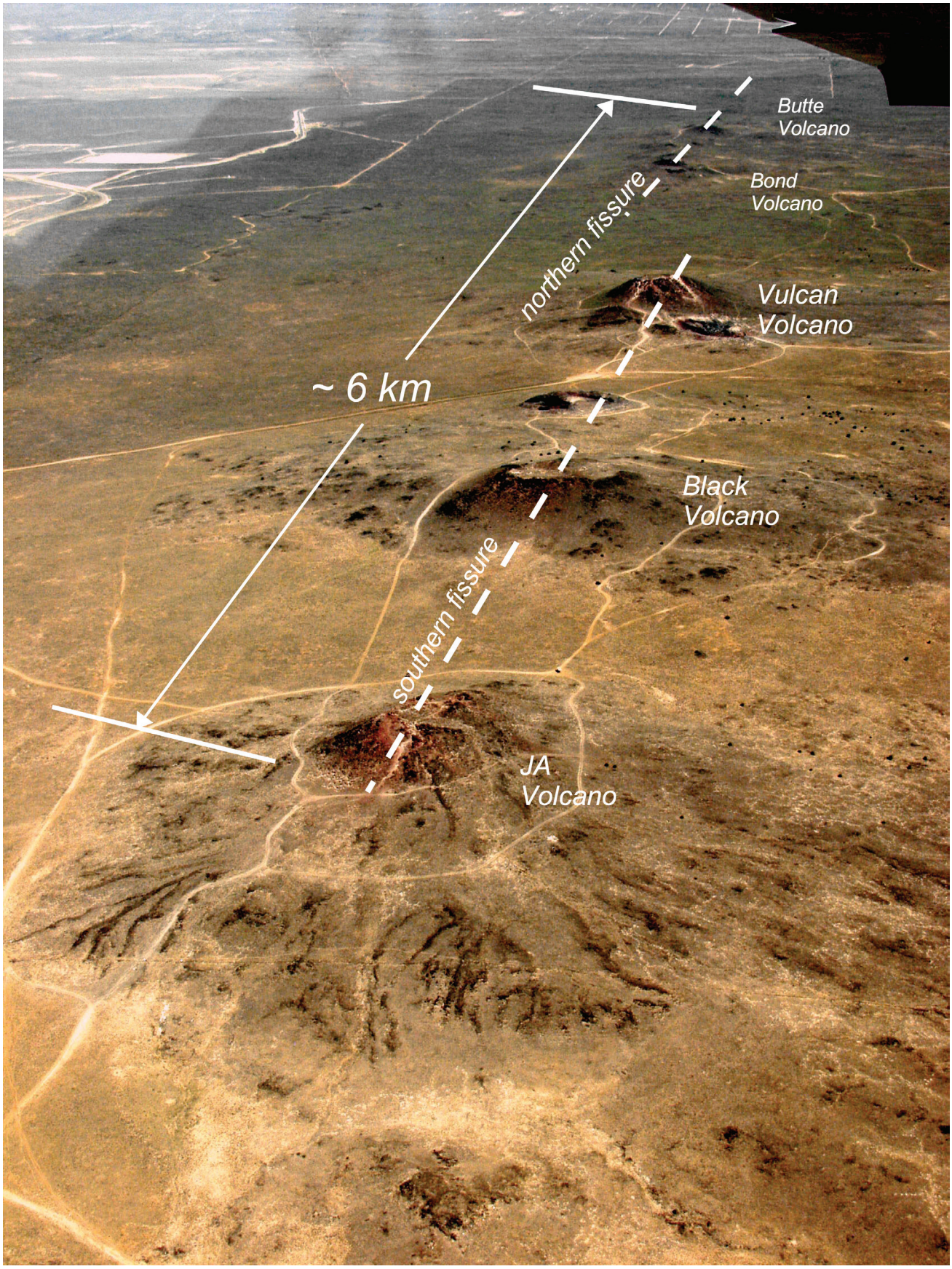


FIGURE 3.17. Aerial view directed north from the southern end of the Albuquerque Volcanoes fissure trend. Two north-trending en echelon fissure segments define a northern and a southern segment. Digitate lavas radial to JA Volcano are typical of late outflows from individual volcanic centers.

and associated flow eruptions probably took place along the entire length of two fissures during the opening phases. These fissures quickly evolved to more centralized vent areas ultimately resulting in the volcanoes we see today. Various observations of the number of vents in the Albuquerque volcanic field have been made by different sources, and the actual number depends on how a volcano is defined in terms of scale and connection with the mantle supply. From the city of Albuquerque, the largest five edifices are most obvious. From south to north these are JA Volcano, Black Volcano, Vulcan Volcano, Bond Volcano, and Butte Volcano (Figs. 3.15 and 3.18). Smaller vent structures occur near Vulcan Volcano, between Bond and Butte Volcanoes, and north of Butte Volcano, and these structures could be considered a volcano depending on the definition used. Each of the five named volcanoes in the Albuquerque volcanic field has a distinct set of features, but all have some form of summit crater, various digitate flank flows, and thin sheet lava-pond spillover flows. Each also had a complex eruption cycle varying between phases of Hawaiian-style effusive eruptions that produced optically dense fire fountains and lava flows and Strombolian pyroclastic phases that produced welded spatter.

Several of the Albuquerque Volcanoes have features that have been described as "caves" on their upper flanks. These are the remnants of large outflow channels typical of vents located on fissures that were roofed by spatter as eruptions progressed. Occasionally, hikers in the winter may notice fog-like vapors rising from some of these caves and wonder whether they are seeing fumaroles, although fumaroles have not been documented here. A more likely explanation relates to thermal insulation within scoria and the highly vesiculated nature of the lava flows. Air emerging from the cave-like openings is supplied by a network of interconnected cavities and tube-like voids within the lava and scoria at depths below where the annual thermal wave penetrates the surface of the land. The emerging air is relatively moist, reflecting a higher moisture content within fractures and small lava tubes within the volcanic edifice. Although this air is cool and damp relative to summer temperatures (~30 °C [~90 °F]), it is warmer and more humid than typical winter ambient air (~7 °C [~45 °F]). When this moist air exits the openings in winter, it condenses in the colder, drier atmosphere, producing wisps of fog that resemble fumarole emissions.

BLACK VOLCANO HIKE

The Black Volcano hike follows the existing trail eastward toward JA Volcano (Figs. 3.18 and 3.20). From JA Volcano, it continues north onto the flank of Black Volcano and ultimately ascends into the Black Volcano crater complex at the summit (Fig. 3.21).

Waypoint 3.04 [N35.1307°, W106.7800°]

Station 1

Station 1 is at the Volcano Day Use Area Trailhead (Fig. 3.15), where we see three of the main cones that make up a north-trending line of cones known as the Albuquerque Volcanoes. The northernmost and most distant is Vulcan Volcano, followed by Black Volcano, and JA Volcano is closest to us and to the east. To understand these landforms, imagine the eruption of JA Volcano consisting of a fire fountain spraying several hundred meters into the air, followed by a decrease in eruptive vigor so that the fountains collapsed into lava pools in the crater and on the adjacent slopes, with lava flowing away in red-hot streams of molten rock. Most visitors do not realize that there has been very little erosion of the volcanoes since the eruptions, assuming that, like at most hiking terrains, the landscape represents considerable erosion of the original volcanic landform. But these features, including small digitate lava flows that form the apron around the base, are constructional volcanic landforms that are close to what they looked like just after the eruptions came to an end.

The trail from the trailhead to the base of JA Volcano crosses early fissure-erupted sheet lava flows. Although most lavas erupted from the fissure flowed eastward toward the Rio Grande valley, a build-up of the fissure axis and the five main volcanic edifices created a slope that sent many flows to the west. These flows have been largely covered by eolian sands blown in from the Llano de Albuquerque to the west, although a few scattered loose samples of the underlying basalt may be encountered along the trail. The extensive eolian cover throughout the volcanic field supports the appearance of significant erosion. In reality, most of these volcanic features are simply covered by eolian sand and dust.

Begin walking up the trail from the parking area toward JA Volcano. Notice that each of the volcanoes has a ramp or apron of lavas around their respective bases. The first outcrops we encounter are digitate lava flows at the base of the apron around JA Volcano. *630 m (2,067 ft)*

Waypoint 3.05 [N35.1286°, W106.7741°]

Station 2

At Station 2, the trail approaches the lower slopes of JA Volcano, where numerous white rocks are exposed along the trail (Fig. 3.18). This white coating is caliche, which is formed by precipitation of calcium carbonate derived from eolian dust (e.g., Van der Hoven and Quade, 2002). The lava flows around Black Volcano are somewhat larger than those from other Albuquerque Volcanoes and tended to pond on the slope, forming a series of steps.

The second rest pavilion, just north of the base of JA Volcano, is on the geographic centerline of a fissure between JA Volcano and Black Volcano. Note that Black Volcano looks flat-topped from this location. This is the rim of the summit crater. As you walk past JA volcanic cone you can see reddish scoria and cinder on the lower slopes. Unlike Black Volcano, JA Volcano has more exposed scoria. These differences reflect the fact that each of the volcanoes has a different architecture despite having a fundamentally similar origin. Both volcanoes have slightly younger flows covering their slopes to the east and west. Scoria tends to be better exposed on the north and south flanks. *150 m (490 ft)*

Waypoint 3.06 [N35.1290°, W106.7718°]

Station 3

At Station 3, the trail turns north at another rest stop with a view of the Rio Grande valley (Fig. 3.18). Here on the fissure line of the Albuquerque Volcanoes, you are standing near the geographic meridian of the Albuquerque Basin. The rift at the latitude of Albuquerque encompasses the area between the Rio Puerco Valley below the western horizon and the Sandia Mountains on the east.

From this waypoint is a view of the Rio Grande valley including the floodplain. This is a good place to consider the diversity of rock ages, geomorphic surfaces, landscapes, and evidences for past and present geologic forces that have shaped the Albuquerque area. The Sandia Mountains can be seen through the saddle to the east between JA and Black Volcanoes, and contain the oldest rocks in the Albuquerque area (1.4 Ga), in contrast to the ~200 ka age of the Albuquerque Volcanoes. To the west, on the horizon, the ~2.5 Ma Mount Taylor composite volcano is visible. The summit of the Mount Taylor amphitheater opens towards us. The two sides and back of the amphitheater crater give the appearance from Albuquerque of a three-peaked mountain.

Continue on the trail northward toward Black Volcano. Lava flows are mostly covered in the saddle between JA Volcano and Black Volcano as a result of burial of windblown sand. As you walk up the trail, keep in mind that the lava flows, scoria, and spatter erupted here are among the most recent volcanic material to be erupted from the fissure and differ from early sheet flow lavas that make up much of the landscape to the east. *275 m (900 ft)*

Waypoint 3.07 [N35.1314°, W106.7712°]

Station 4

At Station 4, we encounter basalt outcrops on the southeast margin of Black Volcano (Fig. 3.18). The upper surfaces of the outcrops form a mosaic of joint blocks 10–20 cm (4–8 in) across. The blocks contain a relatively high number of vesicles generally less than 4 mm in diameter. This is characteristics of the upper 10–20 cm (4–8 in) of basaltic lava flows. The abundance of vesicles implies that the surface of these outcrops within 10–20 cm (4–8 in) to the original surface of the lava flow and there has been little erosion since emplacement, as is typical throughout the Albuquerque Volcanoes. These outcrops have bulbous and irregular morphologies suggesting that they represent lava flows that cascaded down the slopes and experienced local breakouts as they cooled and solidified.

Continue upslope and turn left at the trail leading up the north side of Black Volcano where the trail passes into the summit crater. *315 m (1030 ft)*

Waypoint 3.08 [N35.1332°, W106.7718°]

Station 5

At Station 5, the trail passes through the north rim of the lower of two overlapping summit craters (crater 1 and crater 2; Fig. 3.21). Instead of being a depression, the summit has a flat surface bounded by darker basalt along the margins. The flat surface is likely a result of reddish scoria and volcanic ash that filled the crater during a late-stage Strombolian eruptive phase. The flat floor could also possibly be interpreted as post-eruption infilling the crater by sedimentation. However, observations at Station 9 (see below) indicate that the summit contains minor contributions of eolian sediment that were deposited later. *30 m (100 ft)*

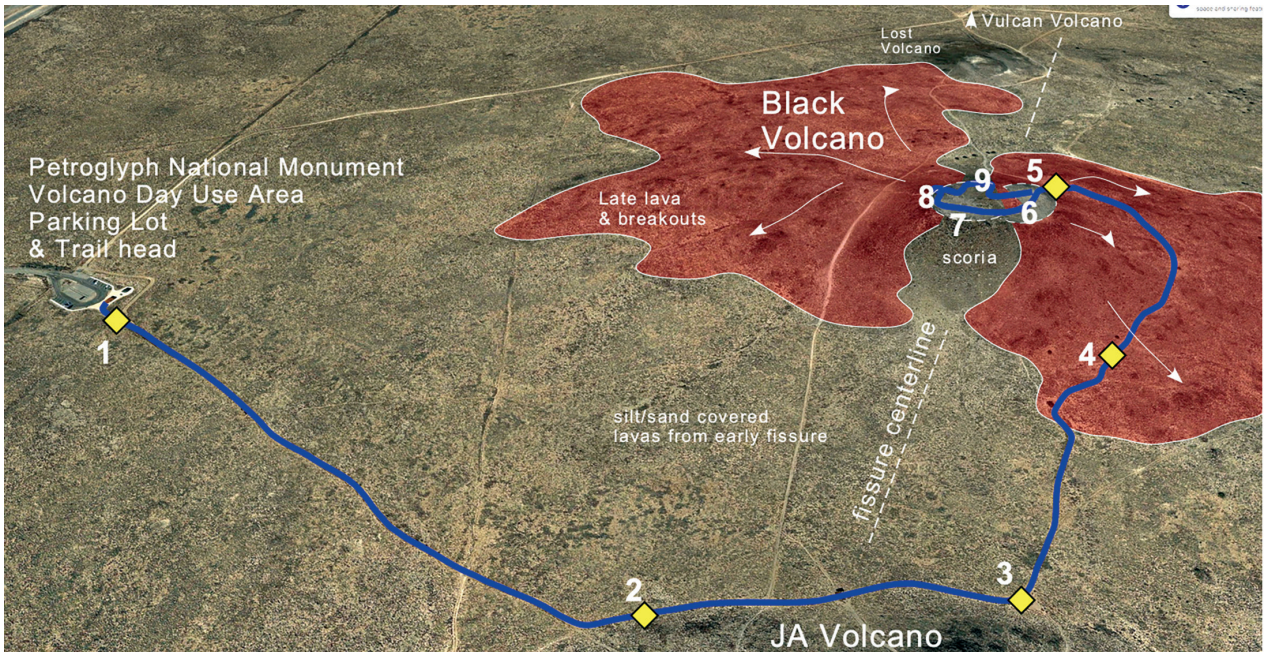


FIGURE 3.18. Overview of the hiking route, including numbered stations described at Stop 2.

Waypoint 3.09 [N35.1330°, W106.7719°]

Station 6

At Station 6, the trail passes through the center of crater 1 (Fig. 3.21). The slope and bench on the right is the marginal rampart of the overlapping, and higher crater 2 to the west. Crater 2 cuts crater 1, indicating that crater 2 is younger. The flat platform within crater 1 consists of scoria and ash from the eruption that continued with crater 2. Scattered blocks and disturbed features on the crater fill are the result of later non-volcanic activity, mostly anthropogenic. *75 m (250 ft)*

Waypoint 3.10 [N35.1325°, W106.7724°]

Station 7

At Station 7, the trail ascends the floor of summit crater 2 (Fig. 3.21). Continue to the south rim for a view back towards JA Volcano and to examine the crater rim outcrops. The basalt here contains good examples of agglomerate (spatter). Scoria are relatively loose ejectites that are highly vesicular. Spatter forms when soft or molten pyroclasts weld together. Agglutinate is a mass of massive to crudely stratified spatter that is typically found close to the vent. Distinctions in the physical character of eruption products are controlled by fluctuations in the balance between gases driving Strombolian activity, supply of new hot magma to the summit vents, eruption rate, and the ballistic paths of pyroclasts.

Filling the crater here, the floor is mostly loose scoria instead of wind-blown sand, soils, and colluvium. Scattered within crater 2 crater are six elongate borrow pits that the remains of efforts to determine the quality of cinders for local construction. The pits churned up the scoria fill to at least a depth of 1–2 m (3–6 ft), implying that the fill is more than superficial. Fortunately for the preservation of the cone, the excavations appear not to have revealed sufficient cinder resources to justify further exploitation. Cinder quarrying did affect other volcanoes. A former small cone immediately north of Black Volcano was quarried and later reclaimed by the National Park Service, and a deep exaction pit on Vulcan Volcano remains from similar early cinder quarrying activity, which was partially reclaimed and restored by the National Park Service.

In addition to the lava flows, spatter deposits, and loose pyroclastics on the summit crater, look for fulgurites. Fulgurites in this area are dark green to black glassy spots around a centimeter in diameter on outcrop surfaces that are the result of



FIGURE 3.19. View of west side of Black Volcano.



FIGURE 3.20. Comparison of JA Volcano with recent Hawaiian eruption center Pu‘u‘ō‘ō illustrating an interpretation of the scale of fire fountaining and style of eruption responsible for the characteristics of JA Volcano.

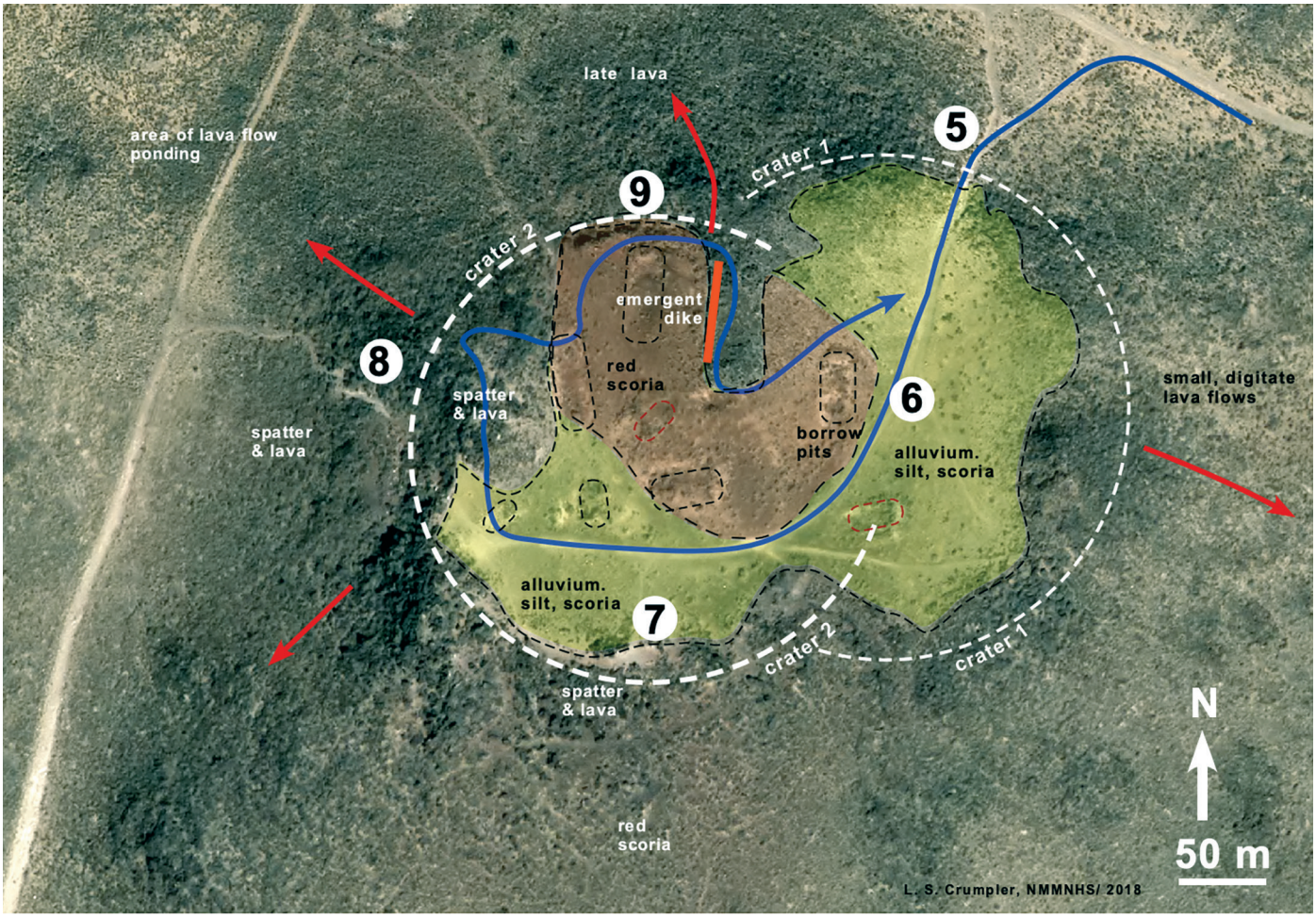


FIGURE 3.21. Geologic sketch map of two summit craters and main characteristics exposed at the summit of Black Volcano. White numbered circles denote station locations.

lightning strikes (Fig. 3.22). As they are the highest features on the West Mesa, these volcanoes have been subjected to numerous lightning strikes over the past 200 ka. In addition to glassy spots on boulders, there are examples in the local soil and loose scoria associated with lightning strikes. *60 m (200 ft)*

Waypoint 3.11 [N35.1328°, W106.7728°]

Station 8

The west rim of crater 2 is the highest point on Black Volcano (Fig. 3.21)**.** This is a good place to view most of the rift valley. The Sangre de Cristo Mountains may be seen on a clear day to the northeast. To the east is an excellent view of the Rio Grande valley and the eastern margin of the Rio Grande rift, which is framed by the Sandia, Manzanita, and Manzano Mountains. In the distance to the northeast is the San Felipe shield volcano on Santa Ana Mesa. To the left (north) is the rim of the Valles Caldera. To the south, Isleta and Los Lunas Volcanoes are visible in the near distance, and beyond them to the southwest are the Ladron Mountains.

Coarse depositional layers of clastogenic basalt on the western edge and summit of the crater are mostly flat lying, but dip westward on the upper flanks of the volcano. Clastogenic lavas coalesce from the fall out of a fissure eruption (Sumner, 1998). Three meters (10 ft) or so to the west–northwest from the summit, in what appears to be just a chaotic mass of agglomerate outcrops, structures in the lava, especially lava gutters measuring 20–30 cm (8–12 in) in width, are present.

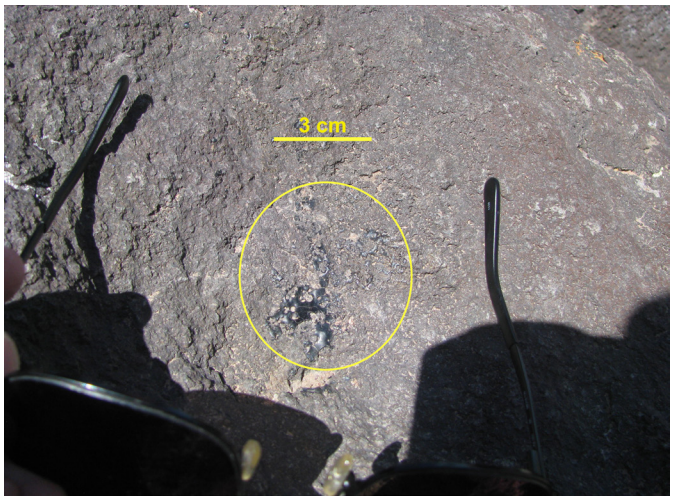


FIGURE 3.22. Example of a fulgurite resulting from a lightning strike on a basaltic outcrop.

Lava gutters are small lava channels originating from clastogenic lava at the base of fire fountains. Larger examples of fountain-fed summit lava ponds and effusive eruptions may produce lavas that flow in large channels between levees. If you look carefully, you will see that each of the volcanoes has numerous examples of lava gutters (Fig. 3.23).

From the summit, the linear alignment of at least the three southern volcanoes (JA, Black, and Vulcan) is notable. The northern two volcanoes (Bond and Butte) are not perfectly aligned along this 6-km (3.7-mi)-long fissure trend (Fig. 3.17). This is because each of the major volcanoes lies on separate shorter fissures that trend at a slightly greater azimuth to the northeast from the main trend line. The alignment of vents that define the overall fissure trend deviates from a northerly orientation by a few degrees (i.e., ~N2E°). The overall fissure trend consists of two distinct and separate en echelon fissure segments, a northern segment that includes Bond and Butte Volcanoes and a southern segment that includes JA, Black, and Vulcan Volcanoes. The southern three principal vents form a northerly alignment (~N5°E) relative to the overall trend of the volcanic field as do the northern vents which strike ~N9°E. Because each of the five principal volcanoes has several smaller vents and fissures, a third fissure trend within each volcano can be identified. For the southern three vents the orientation of fissure elements is northeasterly (~N20°E). For the northern vents, the orientations of the local vent alignments within each vent itself tend to have a more easterly trend. This shift in smaller-scale fissure orientation may reflect rotation of the least principal stress at shallow depths (e.g., Fink, 1985) relative to far-field stresses. To summarize, fissures in the deep crust tend to rotate in strike and splay into shorter fissures in the upper crust due to peculiarities of the strength of rocks.



FIGURE 3.23. Photograph of a lava gutter.

Walk back east–northeast toward the center of the summit crater and toward the piles of red scoria on the margins of the large borrow pit. *60 m (200 ft)*

Waypoint 3.12 [N35.1331°, W106.7723°]

Station 9

Near the center of the summit crater is an unusual fin of basalt within local scoria (Fig. 3.21). The fin is 20–30 cm (8–9 in) wide and trends north for several meters, where it transitions into a lava flow. The fin appears to be plastically deformed as to exhibit an upward-divergent shape. It is likely a near-surface or emergent dike formerly within a small scoria cone that developed within the summit crater during the final stages of eruption. The upper scoria cone has eroded, leaving the resistant dike preserved as a fin. The gradual transition to a lava flow illustrates that the dike fed a small flow emerging from the north end of the scoria cone. The flow preserves volcanic features related to lava emplacement, notably a lava channel approximately 1 m (3 ft) wide floored by wave bands typical of deformation of plastic lava crusts in channels (Fig. 3.24). Like the lava gutters described previously, only larger and with a flat surface, this leveed lava channel represents one of the last events in the eruption of Black Volcano. The slightly rubbly basalt on the channel represents the original surface of a lava stream that solidified in the channel about 200,000 years ago. The emergent dike and associated flow preserve the connection between the source dike and the surface lava flow. The channel continues northward and becomes part of a much larger flow lobe descending the north flank of Black Volcano and onto the surrounding landscape.

Another feature of interest is a vertical cylindrical hole in the lava, about 10 cm (25 in) in diameter, located on the east margin of this channel at its southern end (Fig. 3.25). Concentric bands around the hole on Figure 3.25 indicate this was an original feature of the lava flow. This hole would be a candidate for a tree mold; however, on the summit of a constructional landform, such as an erupting volcano, it is likely a result of fumarolic activity. In this case, the fumarole probably formed over the buried northern tip of a feeder dike that was degassing at the time. Finally, the overall ~N15° orientation of the dike and fissure is another example of small-scale fissures within individual volcanoes generally paralleling the orientation of the larger Albuquerque Volcanoes fissure rotating in strike from the overall north trend of the large-scale fissure.

End of Stop 2

Return to Trailhead parking area along same route. Trace route back to Atrisco Vista Boulevard NW.

0.0 **REZERO ODOMETER before turning right onto Atrisco Vista Boulevard NW.** *0.5*

0.5 Runway for Double Eagle II Airport on left (west). To the right are low topographic features, up to 3–6 m (10–20 ft) tall, in the lava flows called tumuli. Tumuli (tumulus in singular) are dome- to ridge-shaped structures that form on lava flows by localized inflation of a partially solidified crust. They develop when continued lava supply within flow interiors is impeded or redistributed, causing molten lava to pond beneath a rigid to semirigid crust and generate sufficient internal pressure to deform the surface upward. Inflation produces convex uplifts commonly accompanied by axial or radial fractures, crestal fissures, and marginal squeeze-ups where lava is extruded through fractures. Tumuli are common in pāhoehoe flows that have been emplaced on gentle slopes with moderate effusion rates, where lava is transported more efficiently through insulated sheet flows and lava tubes. Their size, shape, fracture patterns, and internal structure reflect the interplay among lava rheology, effusion rate, cooling history, and crustal strength, and they provide constraints on emplacement dynamics and internal flow processes in basaltic volcanic systems (e.g., Walker, 1991).

Basaltic lava flows on the right (east) are part of older flow units of Thompson et al. (2020a). These lava flows could have been emplaced over durations as short as months to years, so this flow may be only slightly older than other flow units. The Butte and Bond cones on right. *1.4*

1.9 Entrance to Double Eagle Airport II on left. *2.1*

3.0 Shell West Mesa Federal #1-24 well was drilled to the northeast. This well drilled through 2,603 m (8,540 ft) of Santa Fe Group basin fill and ended at a depth of 5,906 m (19,375 ft) below land surface (Fig. 3.26; Lozinsky, 1994; Connell, 2011). *0.4*

3.4 Tumuli on right form rough surface texture on flow (Fig. 3.27). Beyond this flow are the northern vents of the Albuquerque Volcanoes. *0.6*

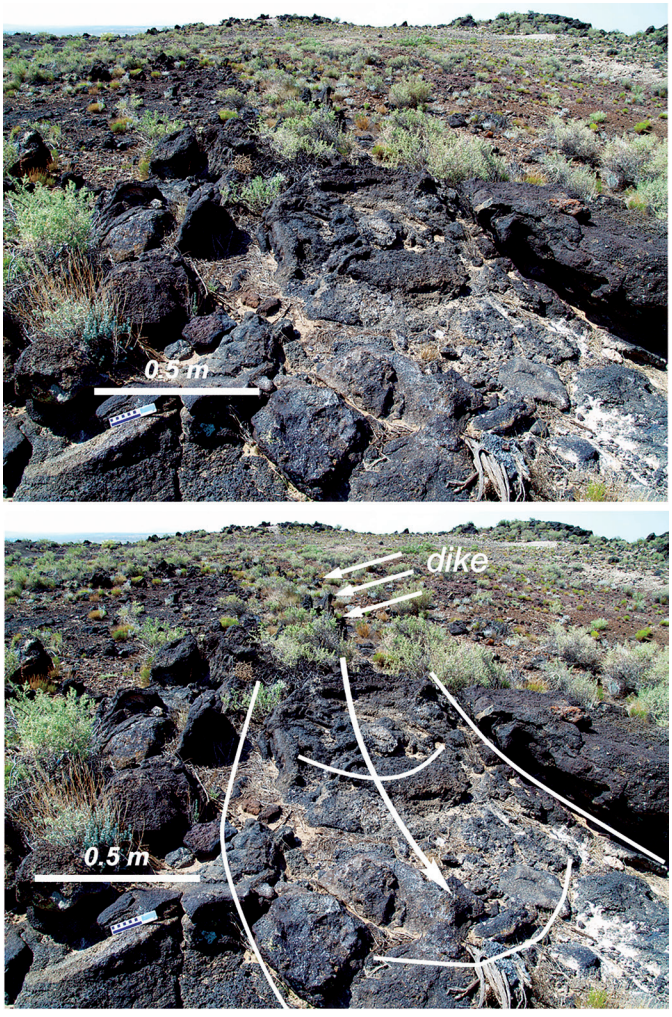


FIGURE 3.24. Lava channel and its feeder dike near station 9. Uninterpreted photograph on the top of figure; interpreted photograph on the bottom.



FIGURE 3.25. Hole formed by a fumarole on the margins of the lava channel illustrated in Figure 3.24.

4.0 Pass intersection of Atrisco Vista Boulevard with Paseo del la Mesa Road. The later road leads east to the Ruth Eisenberg Trailhead. View ahead of tributaries to Arroyo de las Calabacillas, the principal drainage of northwestern Albuquerque and most of the city of Rio Rancho. *0.5*

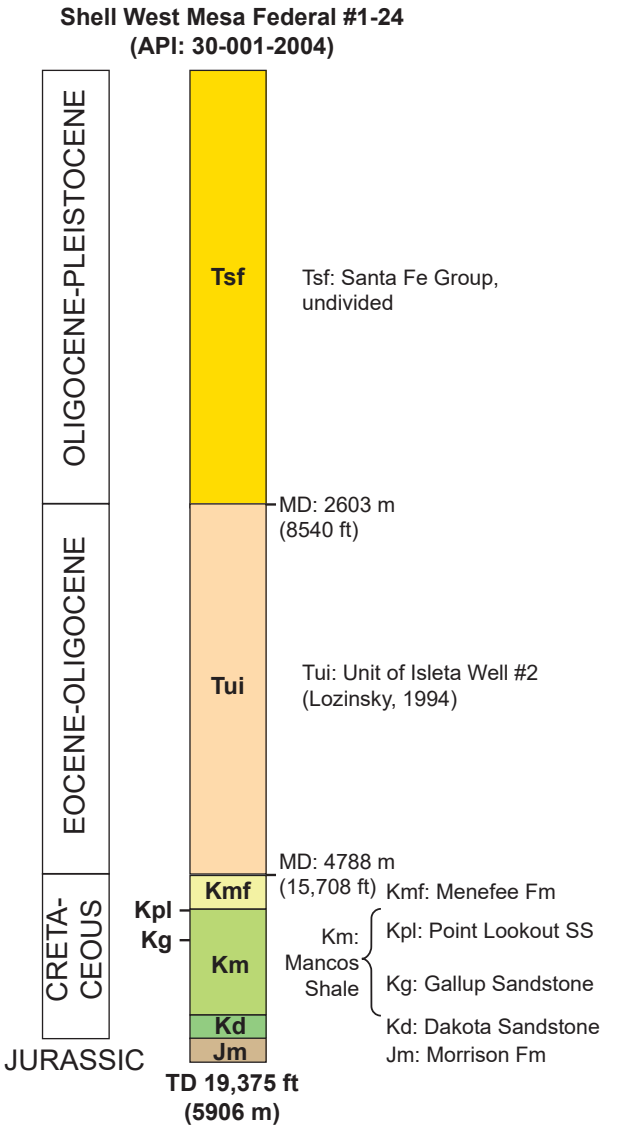


FIGURE 3.26. Shell West Mesa Federal #1 well (API 30-001-20004) drilled through 2,603 m (8,540 ft) of Santa Fe Group basin fill and ended at a depth of 5,506 m (19,375 ft or 3.7 mi) below ground surface (Lozinsky, 1994; Connell, 2011).

4.5 Atrisco Vista Boulevard bends right (east) and becomes Paseo del Norte Boulevard NW. Sandia Mountains form the skyline ahead. The mountains are a footwall uplift that marks the eastern structural margin of the Albuquerque Basin. To the north and east, the Llano de Albuquerque surface is eroded by tributaries of Arroyo de las Calabacillas. *0.7*

5.2 Cinder and aggregate quarry in basaltic lava flows. We are traveling on the oldest lava flow of the Albuquerque Volcanoes, which is capped by 1–2 m (3–6 ft) of fine-grained eolian sand and sheetwash sediment. *0.8*

6.0 Cross intersection with Woodmont Avenue NW. *0.7*

6.7 Cross intersection with Rainbow Boulevard NW. *0.5*

7.2 Cross intersection with Universe Boulevard NW. Koning et al. (2026a, 2026b) inferred a buried fault trending subparallel to Universe Boulevard based on structural contouring of three subsurface stratigraphic datums in the Santa Fe Group. The inferred fault follows an aeromagnetic lineament shown in Grauch and Connell (2013) and likely projects towards a zone of unnamed faults of Star Heights (see Day 2 road log). Groundwater levels and geochemical composition differ across this buried feature, suggesting it may act as a barrier to westward groundwater flow from the Rio Grande (Koning et al., 2026a, 2026b, 2026c). *0.2*

7.7 **Turn right (south) onto Unser Boulevard NW.** *0.3*

8.0 View ahead of aligned volcanic vents. *1.0*

9.0 Pass intersection with Compass Drive and Rainbow Boulevard NW. *0.8*

9.8 Roadcut through 8–11 m (25–35 ft) of massive to sheet-like pāhoehoe lava flows. *0.3*

10.1 **Turn left onto Atrisco Drive NW.** *0.3*



FIGURE 3.27 Photograph of tumulus near northern end of Albuquerque Volcanoes.

10.4 Turn right to entrance to Boca Negra Canyon Day Use Area and drive to parking area to the right. We are in Petroglyph National Monument. Rock collecting is prohibited. Do not bring a rock hammer and stay on marked trails. Walk about 243 m (800 ft) to the east along the north side of loop road and assemble near restrooms.

Waypoint 3.13 [N35.1607°, W106.7197°]

OPTIONAL STOP 3. Boca Negra Canyon, Petroglyph National Monument.

VESICLE CYLINDERS

At this stop, we will explore vesicle cylinders and associated volcanic features in the basaltic lava flows of the Albuquerque Volcanoes (Fig. 3.28). Refer to Goff (2026) for descriptions of vesicle cylinders and associated features. Vesicle cylinders form when water-rich, mafic lava stops flowing. As the lava cools, it solidifies from the bottom up into the interior. This concentrates water at the lower solidification front in the lava's interior, locally allowing large quantities of vapor to form, which generates gas-rich differentiated melt that form vesicles and rise as buoyant plumes or diapirs up from near the bottom of the flow. This process is known as vapor differentiation. Vesicle cylinders grow in diameter upwards as more gas and differentiated liquid fills the plume. Vesicle cylinders can form within a few days of lava emplacement but before development of columnar joints. Vesicle cylinders are not vesicle pipes, which are small vertical tubes that form by steam escaping into the flow bottom from underlying saturated ground. Return to parking lot.

End of Day 3 Road Log

ACKNOWLEDGMENTS

We thank Petroglyph National Monument and the city of Albuquerque Open Space Division for access.

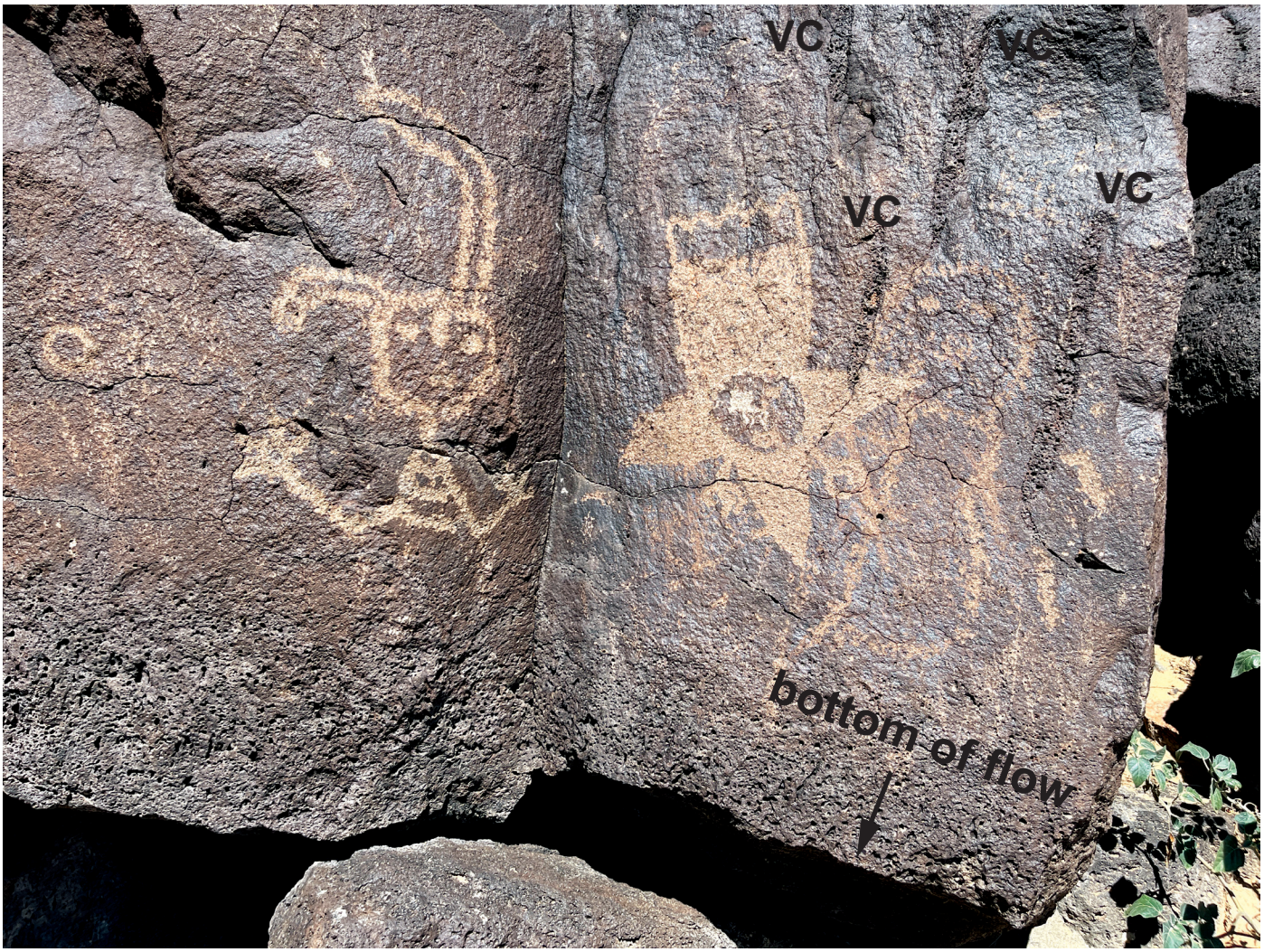


FIGURE 3.28. Photography of petroglyphs carved onto a fallen block of basalt along Boca Negra Canyon Trail. Four near-vertical (relative to original flow-top orientation) vesicle cylinders (VC), which are approximately 4 cm in diameter are visible on upper right face of the block. Vesicle cylinders are commonly elongate and elliptical because columnar jointing develops later in the cooling process. A dark-gray patina of desert varnish obscures many vesicle cylinders, but provides a suitable surface for making petroglyphs.



Cactus Wren (*Campylorhynchus brunneicapillus*) perched on a Tree Cholla (*Cylindropuntia imbricacta*). Spiny plants are a requirement of the Cactus Wren's habitat. Photograph courtesy of Celestyn Brożek.



Sunset filtered through a Tree Cholla (*Cylindropuntia imbricacta*) along the foothills of the Sandia Mountains. Tree Cholla grows at elevations between 1,600 and 1,750 m (~5,250–5,750 ft) in Arizona, New Mexico, Kansas, Texas, Oklahoma, and Mexico. Photograph courtesy of Celestyn Brożek.

New Mexico Geological Society Guidebook, 76th Fall Field Conference, 2026, p. 111–114, https://doi.org/10.56577/FFC-76.111

MINIPAPER:

A SUMMARY OF SURFICIAL GEOLOGIC CONSTRAINTS ON SITE SELECTION FOR MANAGED AQUIFER RECHARGE IN THE ALBUQUERQUE BASIN

Daniel J. Koning[1], Alex J. Rinehart[2], Colin T. Cikoski[3], and Andrew P. Jochems[4]

[1]New Mexico Bureau of Geology and Mineral Resources, 801 Leroy Place, Socorro, NM 87801; dan.koning@nmt.edu
[2]Earth and Environmental Science, New Mexico Institute of Mining and Technology, 801 Leroy Place, Socorro, NM 87801
[3]Wyoming State Engineer's Office, 715 E Roosevelt, Riverton, WY 82501
[4]New Mexico Environment Department, 5401 Watson Drive SE, Albuquerque, NM 87106

Managed aquifer recharge (MAR) encompasses a range of engineering approaches designed to replenish aquifers and store water underground for future use. The Albuquerque Bernalillo County Water Utility Authority (Water Authority) included MAR in its long-range plan, known as "Water 2120," which detailed resource-management strategies that accommodate population growth and drought resilience (Water Authority, 2016). After Water 2120 was adopted in 2016, the Water Authority initiated studies to evaluate and expand MAR capacity. In 2018–2019, the Water Authority funded a study by the New Mexico Bureau of Geology and Mineral Resources to identify optimal locations for recharging the regional Santa Fe Group aquifer system using Rio Grande water during periods of excess supply (Koning et al., 2019). This minipaper summarizes the principal findings of that study.

Two recharge strategies were evaluated: (1) shallow recharge, where water is spread on the land surface or injected into shallow wells above the water table to infiltrate downward into the regional Santa Fe Group aquifer system, and (2) deep injection, where water is introduced directly into the saturated Santa Fe Group aquifer through deeper wells. A GIS-based weighted overlay analysis using a grid size of 100 x 100 m (328 x 328 ft) was used to evaluate recharge suitability for each approach. Shallow-recharge suitability incorporated surface and near-surface parameters such as soil-hydraulic conductivity, drainage characteristics, slope, and the hydrogeologic properties of the upper aquifer. The deep-injection analysis considered many of the same hydrogeologic parameters, but excluded surface conditions and instead emphasized aquifer transmissivity, thickness of saturated permeable units, and existing water-supply well density. Exclusionary buffers were a priori assigned to the Rio Grande floodplain (due to potential for injected water to reach the river or induce swamping) and for known groundwater-contamination sites. For the deep-injection MAR suitability map, an exclusionary buffer zone was also drawn along major faults since they can act as barriers to subsurface flow. These analyses required development of a three-dimensional hydrostratigraphic model of stacked Santa Fe Group units and post-Santa Fe Group units to characterize aquifer geometry and permeability distribution (Fig. 1).

The shallow-recharge suitability map (Fig. 2) classified areas as low, moderate, or high suitability, with some regions considered unsuitable for MAR based on the above-mentioned parameters. The most favorable area for shallow recharge extends from north of Central Avenue to Paseo del Norte Boulevard, and between the Rio Grande floodplain and Eubank Boulevard. High MAR suitability in this area reflects the presence of thick, sandy Plio–Pleistocene deposits of the ancestral Rio Grande that provide highly permeable pathways for infiltration and saturated-zone flow. The deep-injection suitability map is shown in Koning et al. (2019).

Potential geotechnical hazards associated with hydrocompactive (collapsible) soils were also evaluated because these materials can undergo significant volume reduction when wetted, potentially causing ground subsidence and structural damage. Although direct mapping of collapsible soils is difficult, susceptibility was estimated using a GIS-based proxy analysis that integrated soil properties (texture, taxonomic order, suborder, and great group; Soil Survey Staff, 2014), regional landform and geomorphic-surface-age mapping (Hawley et al., 2005), and surface and subsurface geologic mapping of the Albuquerque metropolitan area (Connell, 2008). The resulting susceptibility map (Fig. 3) classified areas having low, medium, high, or extreme susceptibility. High-susceptibility areas correspond to known occurrences of collapsible soils, such as along Tijeras Arroyo and in parts of the Northeast Heights (east of Interstate 25 and north of Central Avenue), and to geologically young fan deposits where hydrocompaction potential may be significant. Uncertainty was evaluated based on the number of contributing model layers (Koning et al., 2019).

Together, the three-dimensional hydrostratigraphic model, suitability analyses for shallow recharge and deep injection, and collapsible-soil susceptibility assessment provide an integrated geologic and hydrogeologic framework for evaluating MAR potential in the Albuquerque area east of the Rio Grande. The results identify areas where permeable ancestral Rio Grande deposits provide favorable conditions for infiltration while also highlighting locations where shallow groundwater or geotechnical constraints may limit recharge feasibility. These datasets provide a foundation for Water Authority planning that can guide site selection, engineering design, and risk mitigation for MAR projects in the Albuquerque Basin.

REFERENCES

Albuquerque Bernalillo County Water Utility Authority, 2016, Securing our water future: https://www.abcwua.org/your-drinking-water-water-resources-mgt-strategy/ (accessed March 2026).

Connell, S.D., 2008, Geologic map of the Albuquerque-Rio Rancho metropolitan area and vicinity, Bernalillo and Sandoval Counties, New Mexico: New Mexico Bureau of Geology and Mineral Resources Geologic Map GM-78, scale 1:50,000. https://doi.org/10.58799/GM-78

Hawley, J.W., McCraw, D.J., Love, D.W., and Connell, S.D., 2005, Map of surficial materials of New Mexico: New Mexico Bureau of Geology and Mineral Resources, Open-file Geologic Map 295, scale 1:500,000. https://doi.org/10.58799/OF-GM-295

Koning, D.J., Cikoski, C.T., Rinehart, A.J., and Jochems, A.P., 2019, Mapping suitability for Managed Aquifer Recharge in the Albuquerque Basin: New Mexico Bureau of Geology and Mineral Resources Open-file Report 605, 84 p. https://doi.org/10.58799/OFR-605

Soil Survey Staff, 2014, Gridded soil survey geographic (gSSURGO) database for New Mexico: U.S. Natural Resources Conservation Service (NRCS), U.S. Department of Agriculture (USDA) Database Conterminous US Package: https://gdg.sc.egov.usda.gov/ (accessed April 2017). Updated version of webpage: https://websoilsurvey.nrcs.usda.gov/app/ (accessed March 2026).

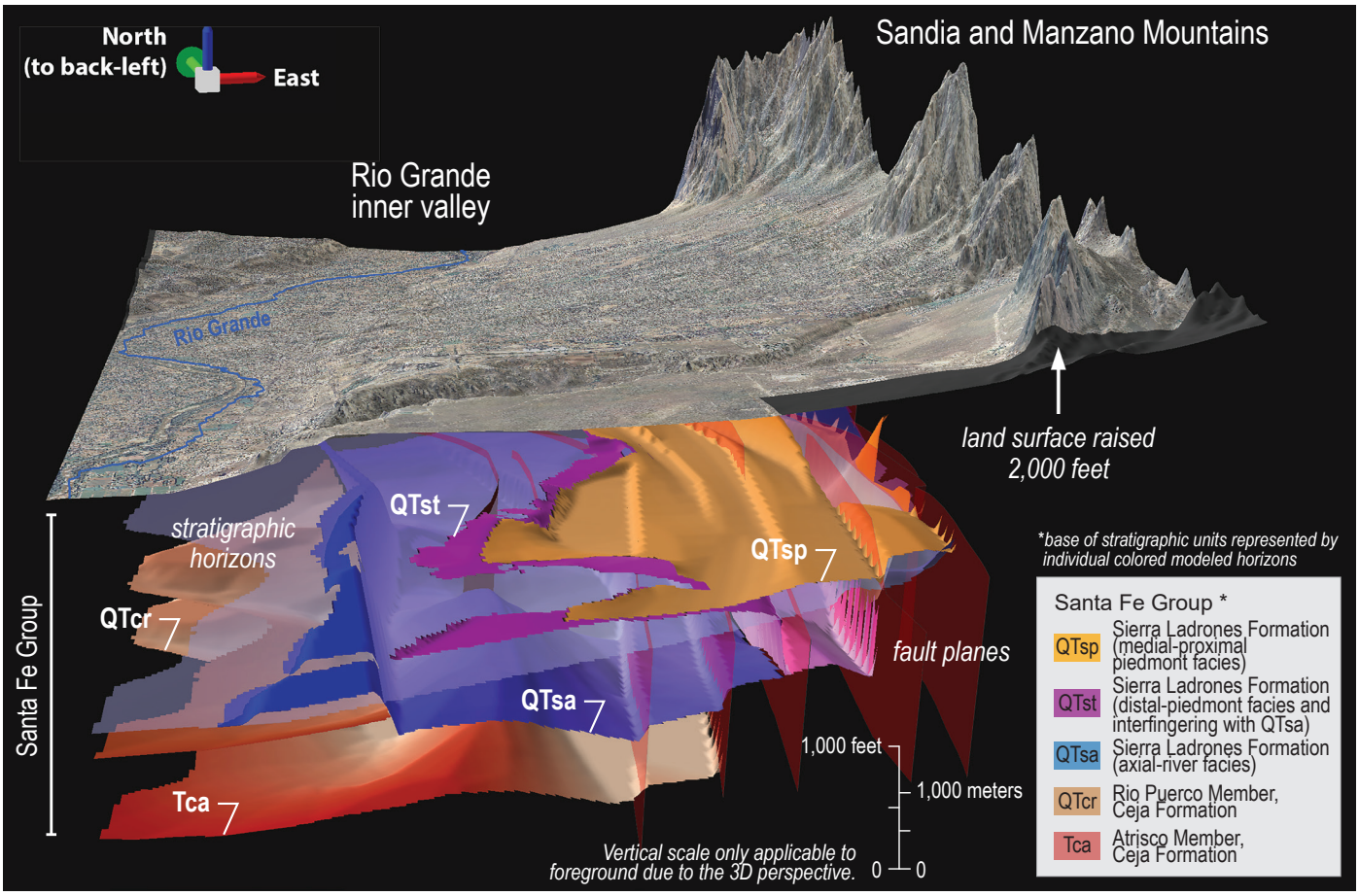


FIGURE 1. Three-dimensional geologic model of the Santa Fe Group. The land surface was raised by 2,000 ft (610 m) and post-Santa Fe Group deposits have been removed for easier viewing of the stratigraphic intervals of interest. Axial-fluvial deposits occur beneath the Atrisco Member but are not shown in the figure because they are below MAR targets in this study.

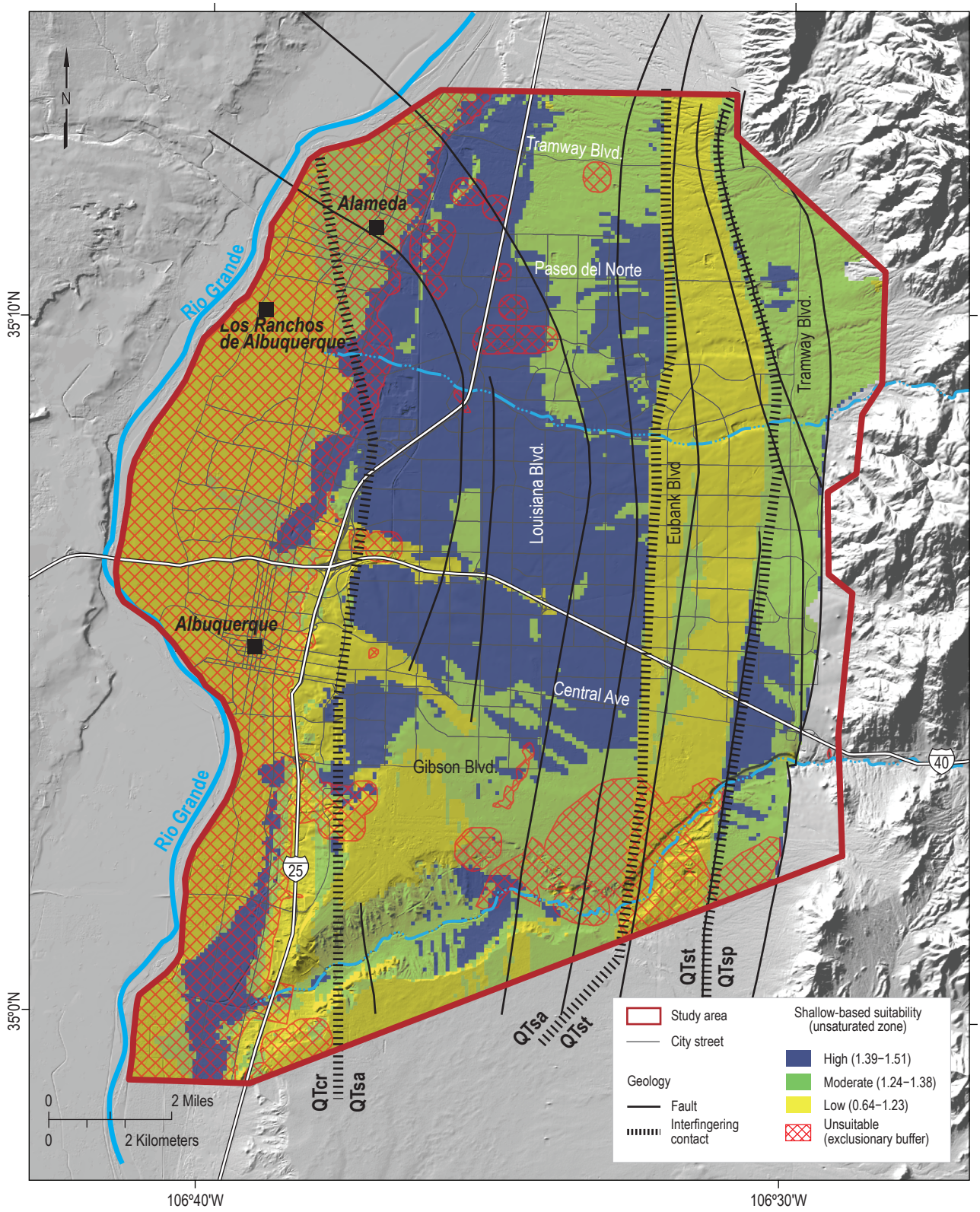


FIGURE 2. Map showing color-coded MAR suitability that permits qualitative assessment of the efficacy of shallow-based recharge. The interfingering contact symbol pertains to units in the upper Santa Fe Group aquifer, which are labeled near the southern study area boundary. Unit QTcr represents the Rio Puerco Member of the Ceja Formation. Other units are part of the Sierra Ladrones Formation and include axial-fluvial facies (QTsa), piedmont facies (QTsp), and a fine-grained transitional zone (QTst) between the axial-fluvial and piedmont facies.

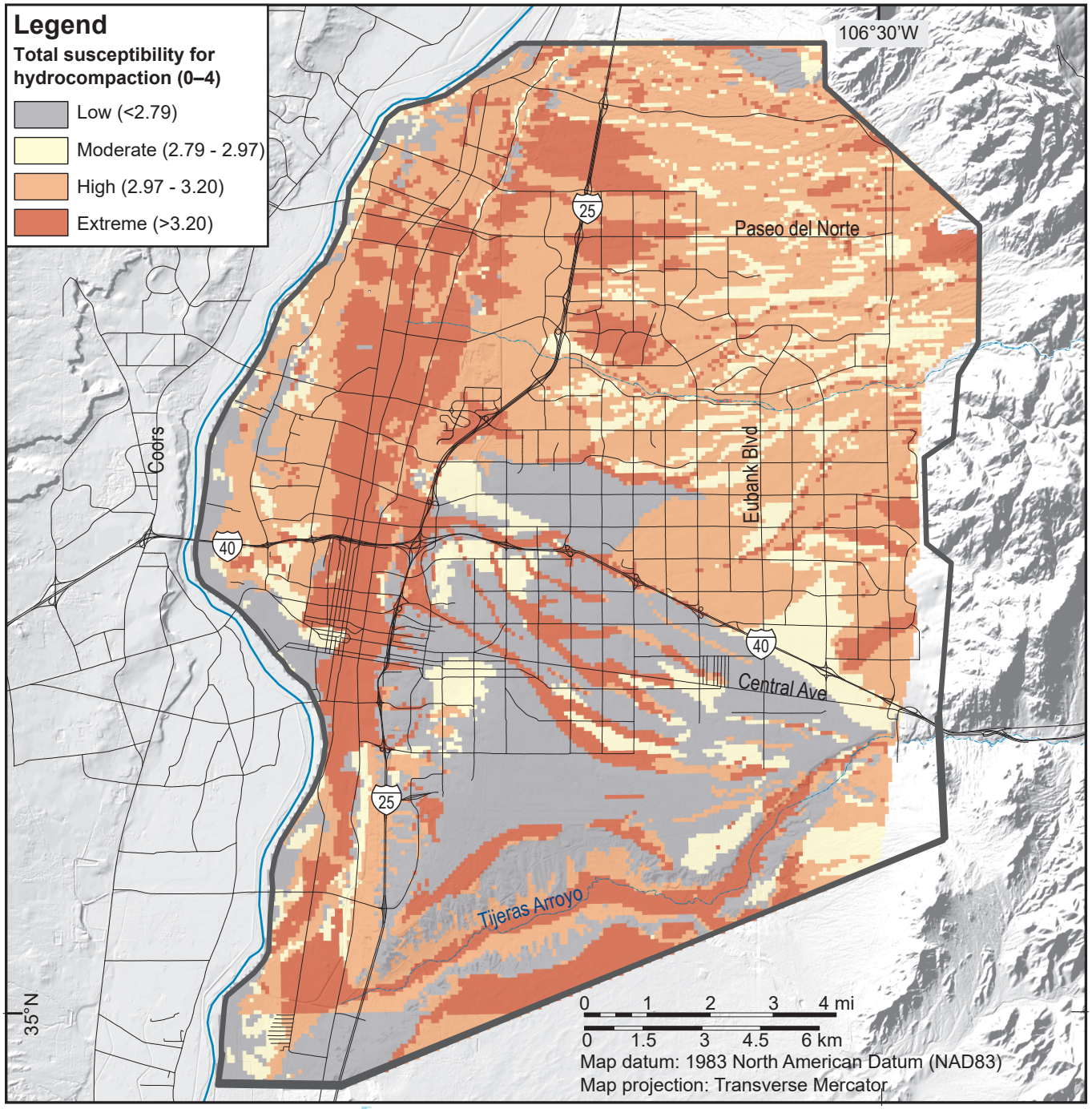


FIGURE 3. Hydrocompactive soils susceptibility map. Susceptibilities were estimated as the average of proxy susceptibilities and range from low, medium, high, and extreme. Low susceptibilities generally correspond to areas of active fluvial deposition (e.g., Rio Grande) and older (Plio–Pleistocene) alluvial fans, whereas extreme susceptibilities correspond to geologically young (Holocene) alluvial fan and valley-border deposits on the outer margins of the modern Rio Grande floodplain or to Rio Grande terraces.